NGU Report 2009.042
Determination of altitude-dependence of standard spectra and stripping ratios for the GR820 Airborne Gamma Ray Spectrometer

NGU
Norges geologiske undersøkelse
Geological Survey of Norway

Geological Survey of Norway
NO-7491 Trondheim, Norway
Tel.: 47 73 90 40 00
Telefax 47 73 92 16 20

REPORT

Report no.: 2009.042 | ISSN 0800-3416 | Grading: Open

Title:
Determination of altitude-dependence of standard spectra and stripping ratios for the GR820 Airborne Gamma Ray Spectrometer.

Authors:
Bjørn H. Heincke, Robin J. Watson, Thomas Møller

Client:

County:

Commune:

Map-sheet name (M=1:250.000)

Map-sheet no. and -name (M=1:50.000)

Deposit name and grid-reference:

Number of pages: 42 Price (NOK): 265,-
Map enclosures:

Fieldwork carried out:	Date of report:	Project no.:	Person responsible:
	11.09.2009	267600	Gun V. Ganerød

Summary:

NGU's Airborne Gamma Ray Spectrometer system is used both for geological mapping, and for monitoring radioactive materials in the event of nuclear emergencies. Traditional methods of processing spectrometer data use channel windows around the radionuclides of interest; more advanced methods make use of the full spectra information. Such advanced methods require prior knowledge of the dependence of standard spectra with height.

Height-dependent measurements have been made using concrete calibration pads, and polythene sheets to simulate the effects of altitude. The height-dependent standard spectra were determined using singular value decomposition and a global inversion scheme. Using the first two eigenimages, together with suitable scaling factors, we were able to recreate the measured height-dependent standard spectra.

The height dependence of standard Th, U and K stripping ratios were also calculated from these standard spectra.

Keywords:			
	Radiometrics (Radiometri)	Geophysics (Geofysikk)	Calibration

CONTENTS

1. Introduction

Although most airborne gamma-ray spectrometers can record at least 256 channels of data over the energy range 0-3 MeV, little of this data is used in traditional processing. The conventional approach to process airborne gamma-ray spectrometric data is to sum the observed spectra over three relatively broad energy windows. These window count-rates are then processed to obtain estimates of potassium (K), uranium (U) and thorium (Th) element abundances. Such data processing includes for example correction of the deadtime, removal of background radiation, stripping of the K, U and Th contributions to the three windows ("unmixing"), and correction of the stripped count rates for the height of the detector (IAEA 2003). An obvious limitation of the three-window approach is that this processing strategy does not use all the information in the observed spectra (Minty 1998). In addition to the concentrations of K, U and Th, multi-channel spectra contain information on (1) the distance between the source and the detector, (2) the contribution of atmospheric radon and (3) the contribution of cosmic radiation to the observed spectrum.

To account for these limitations, more advanced processing strategies using complete spectra have been suggested by different authors (e.g. Minty 1998). This kind of processing requires knowledge of the effect of altitude on the standard spectra of K, U and Th. Such altitude dependent spectra can be determined by performing airborne measurements over ground areas of known concentration. This is often difficult to carry out in practice, however, requiring large areas of land for which ground concentrations are reliably known. Alternatively, ground-based measurements on calibration pads can be carried out, where the effects of air (for specific temperature and pressure conditions) are simulated by the use of suitable absorbing materials (Dickson 1981). As a byproduct of such calibration measurements, the height dependence of the stripping ratios and sensitivities (how the count rates correspond to ground concentrations) can be determined. These are important parameters for improving the accuracy of conventional window-based processing.

At NGU the gamma ray spectrometer system GR820 is frequently used in airborne geological mapping to determine surface concentrations of natural radionuclides, and forms a part of NGU's radiation protection management system (Smethurst et al. 2005; Rønning 2008) for the identification of Caesium contamination in the event of nuclear emergencies. In anticipation of using full-spectrum processing methods in the future, a series of measurements were carried out on NGU's calibration pads to determine the altitude dependence of standard spectra, using polythene sheets to simulate the effects of altitude.

This report describes 1) the height simulation measurements and pre-processing applied to the measured spectra, 2) the determination of height-dependent standard spectra by singular value composition and global inversion schemes, and 3) the determination of height-dependent stripping ratios. Results are compared with literature.

2. Measurements

Calibration measurements to determine the variation of both standard spectra and stripping ratios with simulated height were carried out in front of the goods delivery entrance of NGU in Trondheim. Weather conditions during measurements on 24.09.08 and 25.09.08 were stable, dry and calm.

2.1 Gamma-ray spectrometer system

The gamma-ray spectrometer system is made up of NaI crystals and a GR820 spectrometer. The NaI detector consists of 5 crystals with total volume 20.9 litres. Four crystals (16.7 litres) are configured to be "downward" looking, and one crystal (4.2 litres) configured "upward". The crystals are connected to a 256-channel GR820 spectrometer, with an energy range 0.3 MeV to 3.0 MeV. Data acquisition and visualisation was controlled from a laptop using GAMMALOG LabView software (Smethurst et al. 2005), and acquired spectra were saved to hard-disk for subsequent processing. During data acquisition, stabilisation of the detector system is automatically performed in the spectrometer hardware, using the pronounced and reliable peak of the naturally occurring Potassium-40 radionuclide.

2.2 Calibration pads

A set of four concrete calibration pads (GSC 1987) was used to provide suitable standard spectra for the determination of height dependent K, U and Th spectra and stripping ratios. Three of the pads have increased concentrations of potassium, uranium and thorium, respectively; a fourth pad (the "background" pad) contains around the same amount of potassium as the uranium and thorium pads, the same amount of uranium as the potassium and thorium pads, and the same amount of thorium as the potassium and uranium pads. Each block measures 1m x 1m x 0.3m (Figure 1c).

2.3 Configuration

Measurements were made with each of the calibration pads in turn. The NaI detector was suspended above the calibration pad from a scaffolding frame, with a distance of 23cm between the upper surface of the calibration pad and the lower surface of the detector (Figures 1a and 1b). The relative positions of the NaI detector and the pad were fixed throughout all measurements. The position of the calibration pad was marked on the ground, so that when switching pads, each calibration pad could be positioned at the same location.

To simulate the effect of different flight heights, a number of plastic sheets (1.5m x 1.5m x 12mm) were placed between the pad and the detector during measurements.

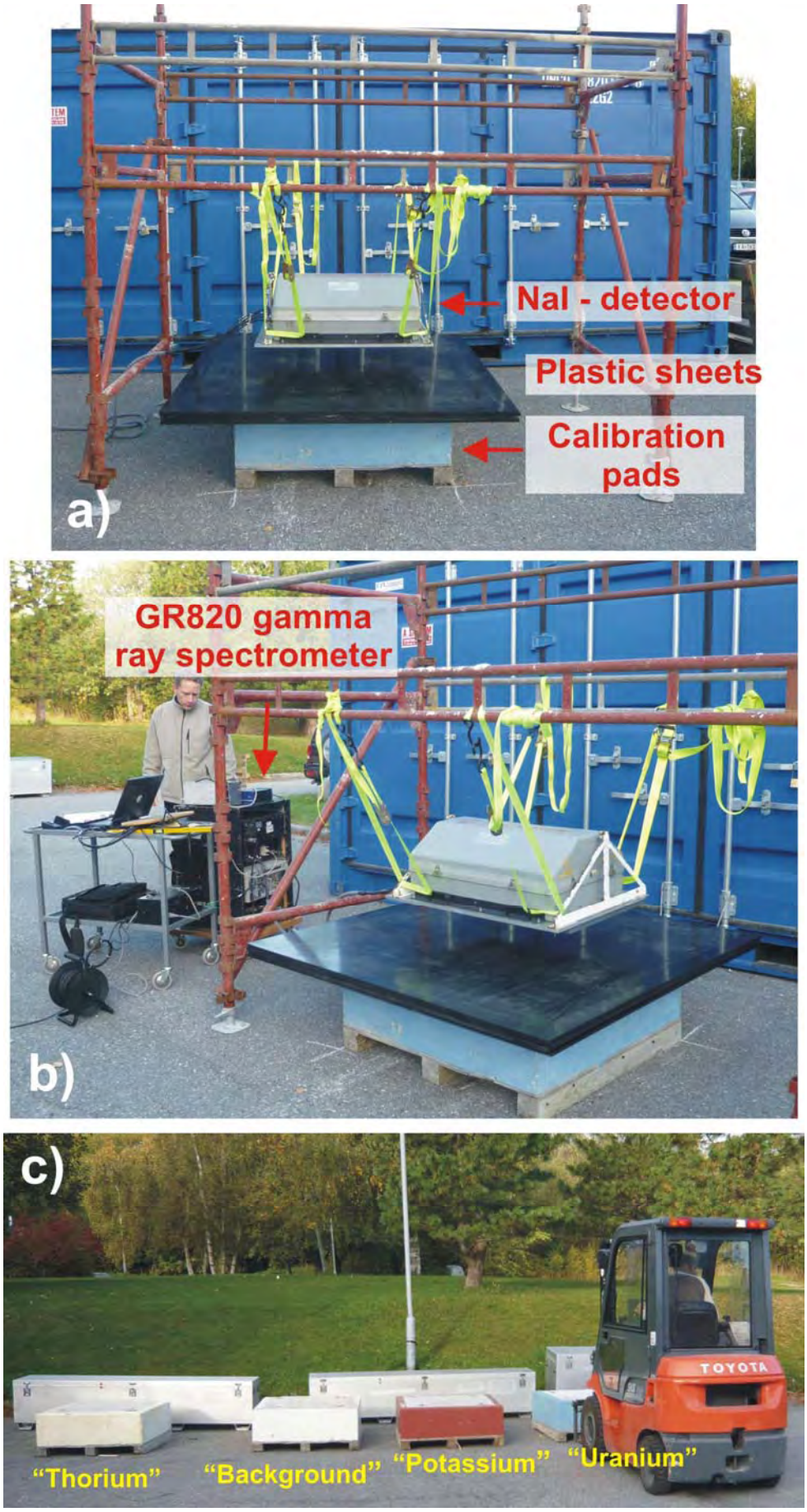

Figure 1: a) and b) illustrate the experimental arrangement for calibration measurements; c) shows the concrete calibration pads, one of which is being manoeuvered by forklift truck.

For each calibration pad, including the background pad, measurements were performed with 0, 1, 2, 4, 6 and 8 plastic sheets. Each measurement consisted of collecting data over a 5 minute period. Measurements were performed over 2 days in the following sequence:

Day 1: Background pad – measurement 1
Potassium pad
Thorium pad
Background pad – measurement 2

Day 2: Background pad – measurement 3
Uranium pad
Background pad – measurement 4

3. Processing

Spectra were first live-time corrected. For each simulated height, the spectra from the K, U and Th pads were then background-corrected by subtracting an average spectrum from the background pad for the same simulated height. For K and Th spectra, the average spectra of background measurements 1 and 2 were subtracted; for the U spectra, the average spectra of background measurements 3 and 4 were subtracted.

The background spectra include contributions from the unconsidered radioisotopes in the pads, radioactive sources in the surrounding ground, air radon and from cosmic gamma rays. We observed only minor differences in the background spectra measured on the same day (see Figure 2 and Figure 3); as such we can assume that any atmospheric radon and cosmic contributions were approximately constant throughout the measurements and that subtraction of the background spectra reliably remove contributions from air radon and cosmic radiation. The measured spectra from K, U and Th are presented in the Figures 4a, 5a and 6a and the same spectra after live-time and background corrections are shown in the Figures 4b, 5b and 6b.

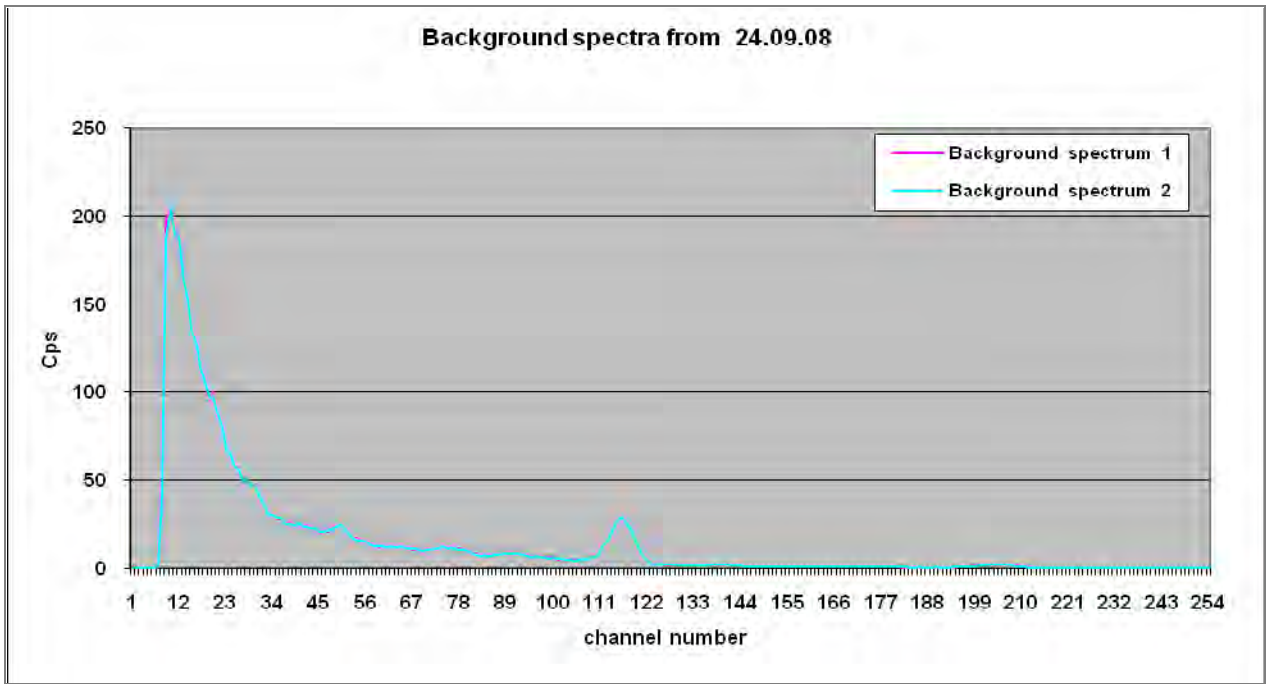

Figure 2: Spectra from the background pad without plastic sheets at day 1. Spectrum 1 was recorded before the Potassium pad measurements, and spectrum 2 after the Thorium pad measurements.

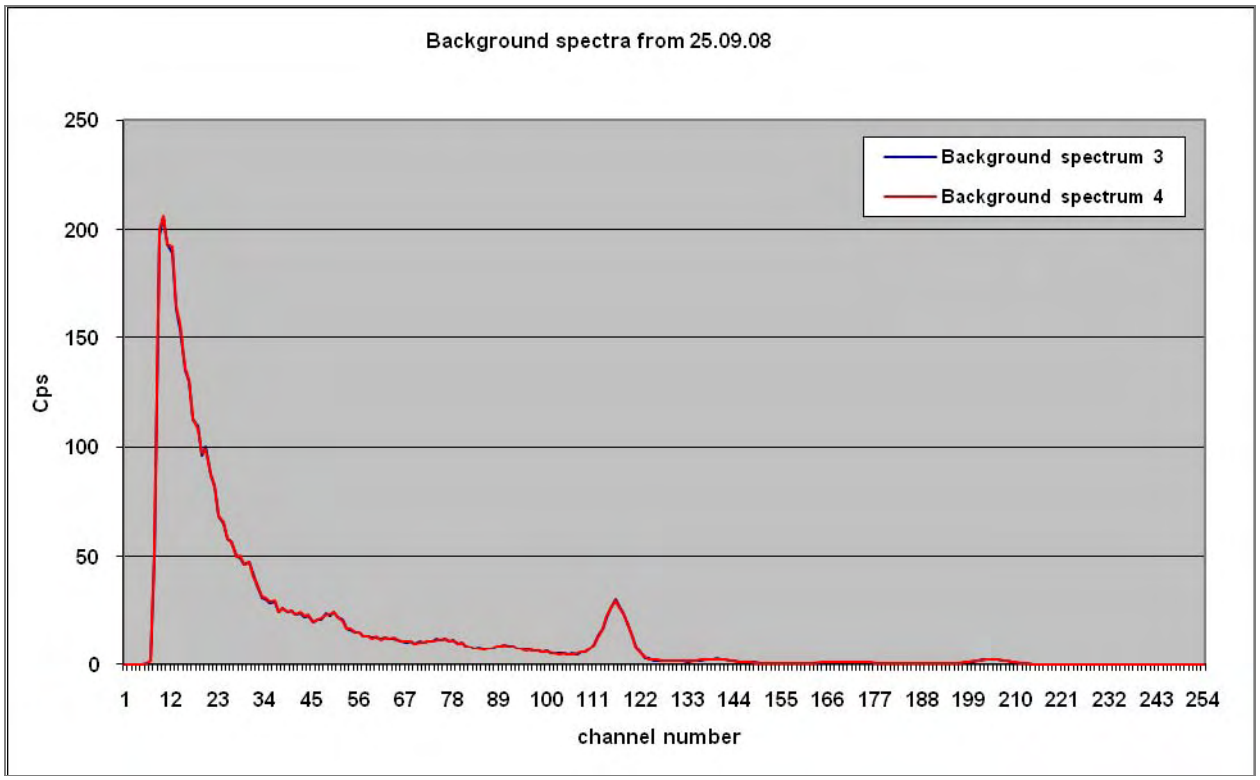

Figure 3: Spectra from the background pad without plastic sheets at day 2. Spectrum 3 was recorded before, and spectrum 4 after, the Uranium pad measurements.

3.1 Geometrical correction

Throughout the simulated height measurements, the detector was situated 23cm above the pads. To correct for the effects of this raised measurement position, a series of correction spectra were determined by comparing the spectra recorded in the raised position with those recorded when the detector was sitting directly on top of the pads. Spectra recorded with the detector directly on the pads were collected by us as part of routine calibration measurements in August 2008.

The height-dependence of standard spectra is non-trivial; compton-scattered and photo-peak contributions will have differing altitude dependencies, and so any given standard spectrum will have its own height-dependent behavior (Bailey 1986, Allyson and Sanderson 1998). In addition to the effects of the detector height, the source-detector geometry changes significantly due to the finite size of the calibration pads, making these geometrical corrections even more complex. We therefore need to calculate geometrical corrections for each standard spectrum.

To calculate this geometrical correction we divided the cps in each channel recorded when the detector was sitting directly on the calibration pads, with those recorded when the detector was suspended above the pads (without any intervening plastic sheets). These correction "spectra" were calculated separately for Potassium, Uranium and Thorium, and a 5-channel median-filter was applied to reduce the effect of random noise. Finally, the correction "spectra" were multiplied channel-wise with each height dependent K, U and Th spectrum. The applied geometrical correction spectra are shown in Figure 4, and the K, U and Th spectra after the geometric correction are shown in Figures 5c, 6c and 7c.

We assume here that variations in spectra related to detector height and source-detector geometry can be described to first order by exponential functions $e^{-\mu x}$ where x is the distance or height of the detector above the ground and μ is the energy-dependent and source-dependent attenuation coefficient. Such exponential functions are nothing more than multiplication factors whose values vary with energy (channel number); therefore we believe that our approach adequately accounts for these geometrical effects to first order.

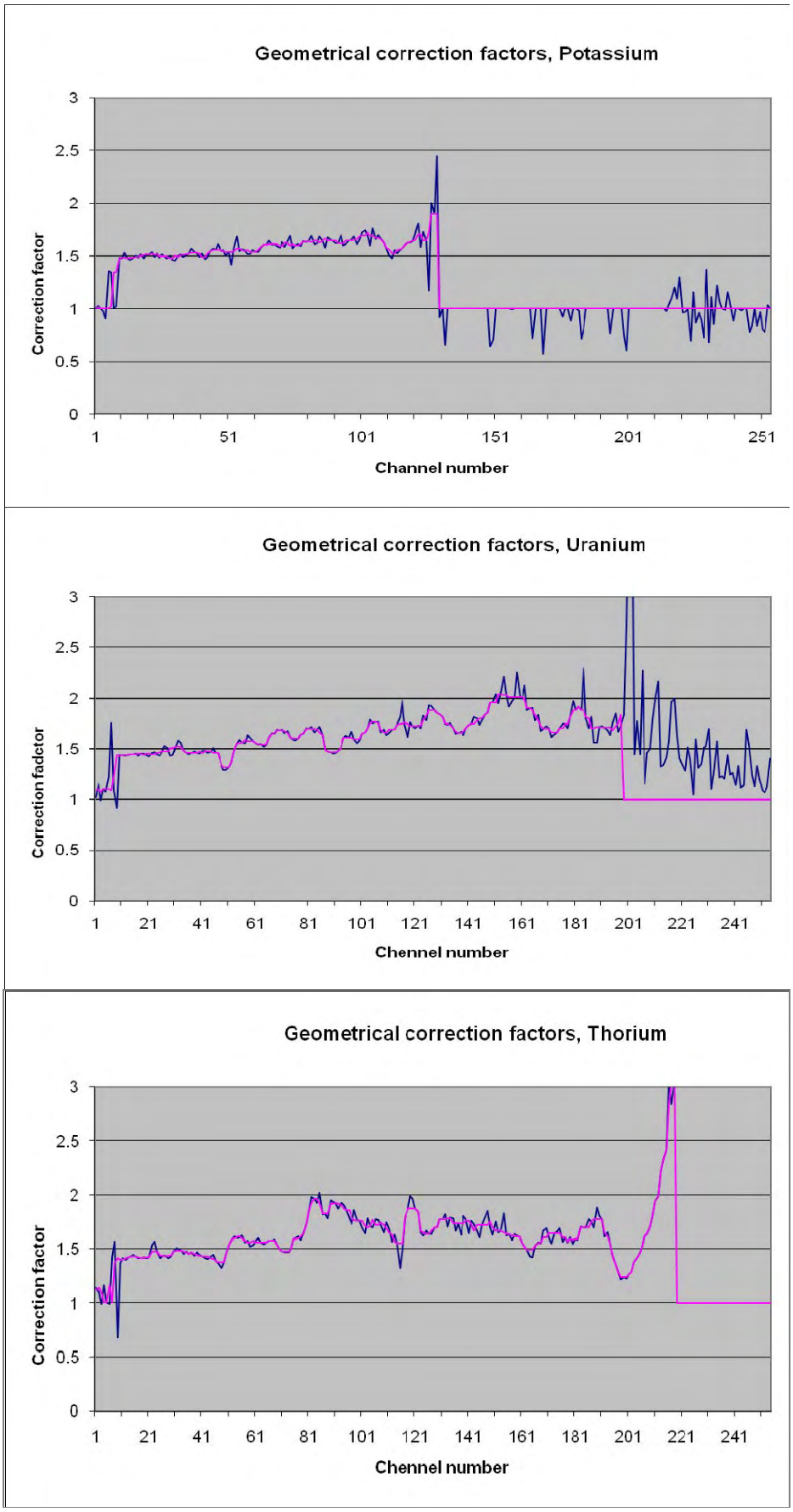

Figure 4: Geometrical corrections factors for the standard spectra of K, U and Th. Raw data (purple) and median-filtered data (pink).

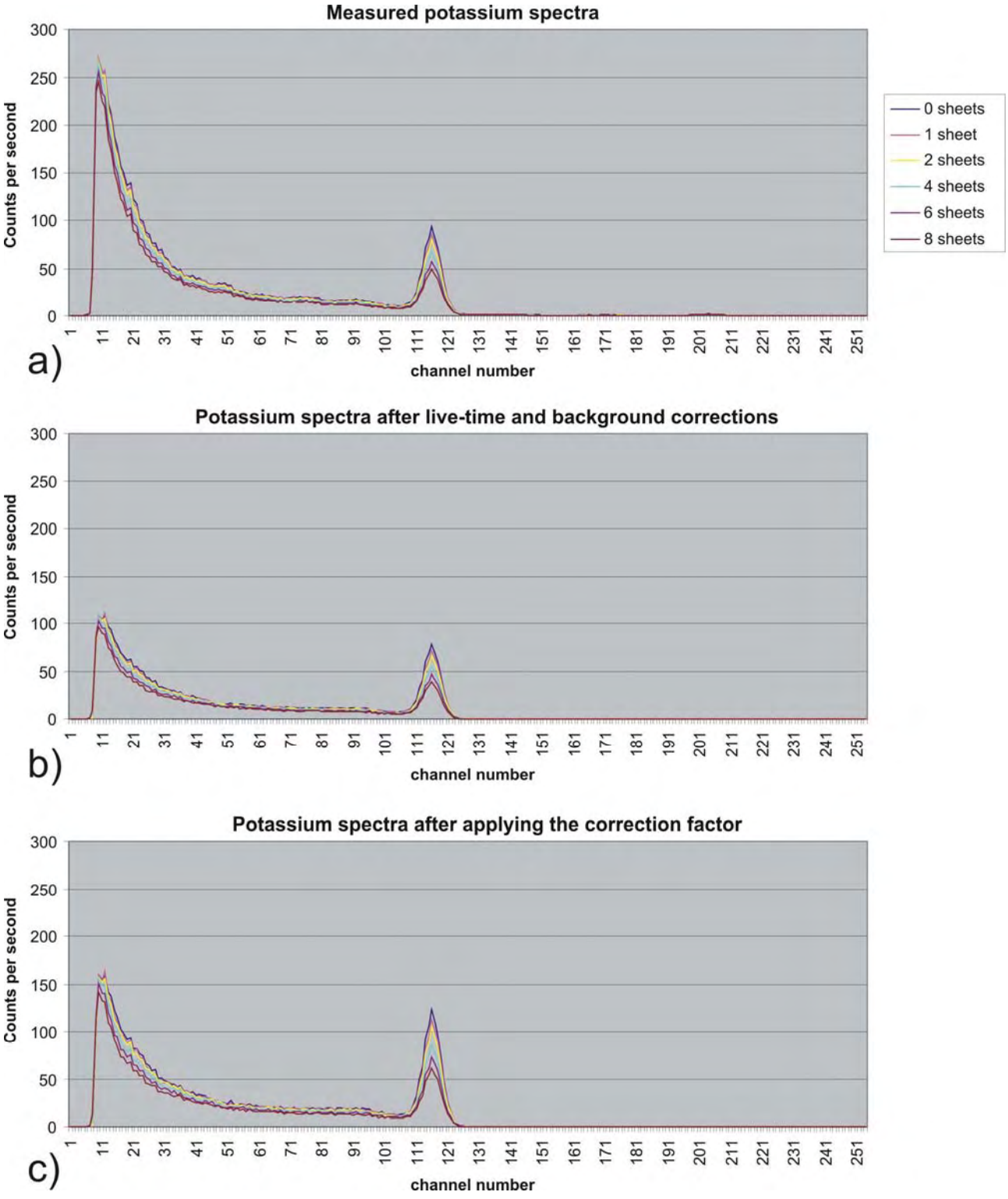

Figure 5: Potassium spectra as a function of (simulated) height, a) before corrections; b) after live-time and background corrections; c) after geometrical corrections.

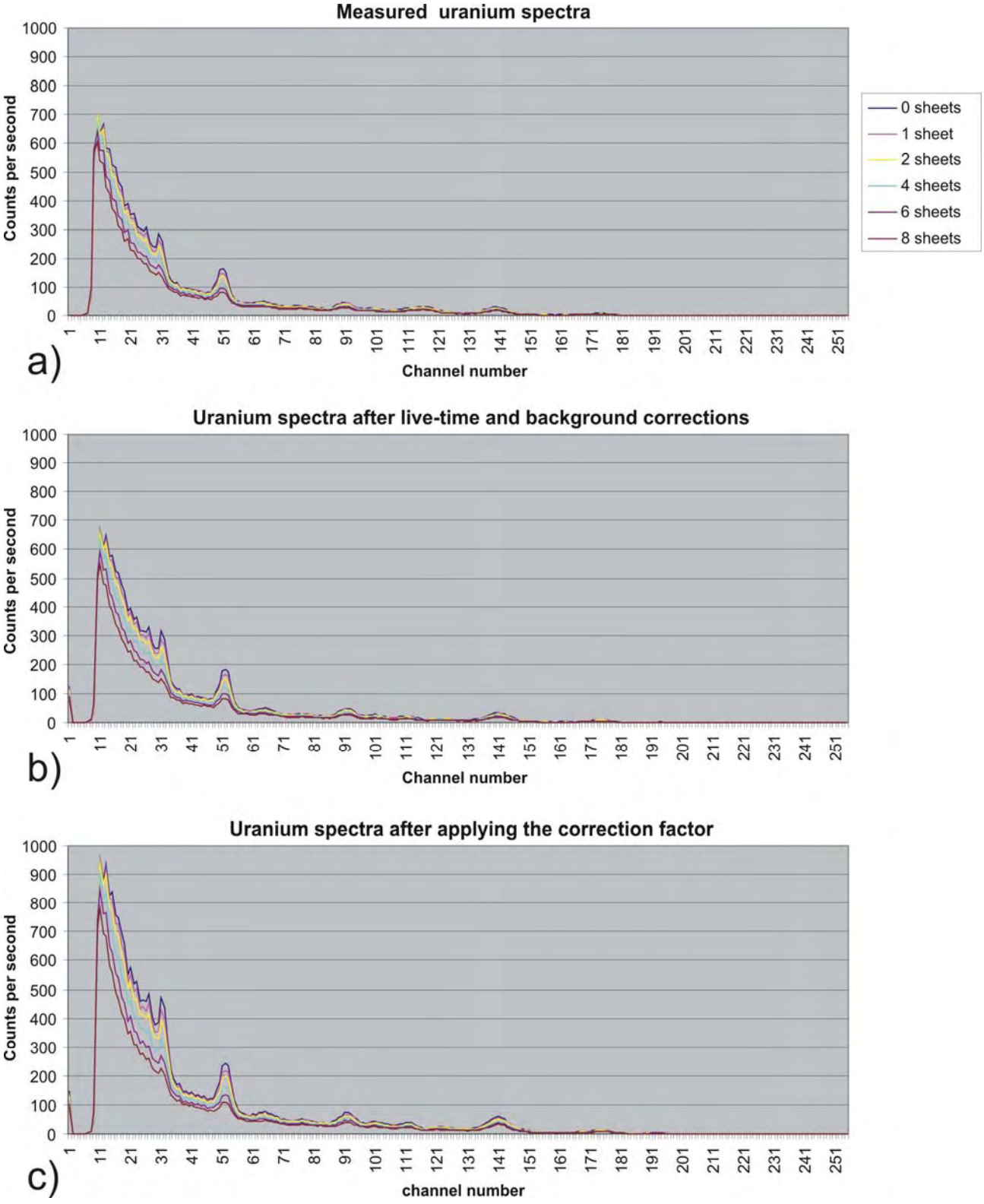

Figure 6: Uranium spectra as a function of (simulated) height, a) before corrections; b) after live-time and background corrections; c) after geometrical corrections.

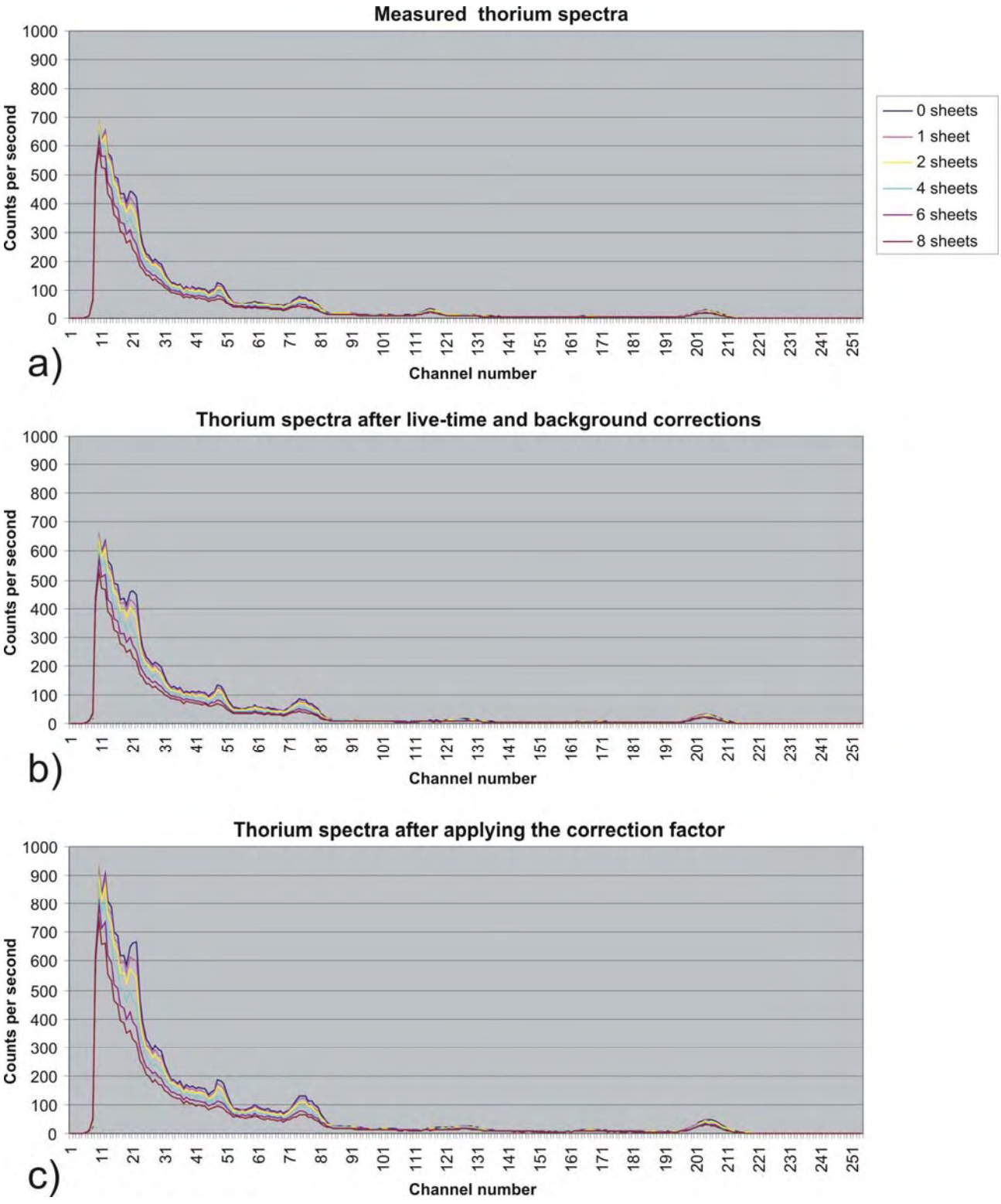

Figure 7: Thorium spectra as a function of (simulated) height, a) before corrections; b) after live-time and background corrections; c) after geometrical corrections.

4. Determining the height-dependence of standard spectra and stripping ratios.

Minty et al. (1998) determined K, U and Th standard spectra for a number of simulated detector heights on calibrations pads. Because these measured spectra were related to a few fixed detector heights, they highlighted that some kind of interpolation was required to determine standard spectra for flexible flight heights. To obtain these flexible standard spectra from a few simulated detector heights they used a method suggested by Dickson (1980), who showed that the height-dependent spectra of each of the three radio elements K, U and Th can be determined by a combination of principal component analysis and a global search algorithm to find adequate scaling parameters. Here we follow a similar strategy to determine the general height dependence of the K, U and Th spectra from our measured height simulated spectra.

4.1 Calculation of simulated altitude

Attenuation effects of spectra with altitude were simulated by placing polythene sheets between the source and the detector. The dominant process of gamma-ray interaction in the relevant energy range is Compton scattering, which is dependent on the electron density in the absorbing material; the electron density of polythene is similar to that of air (see Appendix A). An effective altitude can be assigned to each polythene sheet based on its mass per unit area and electron densities (see for example Dickson (1981) where plywood sheets were used). Hence, a variation in altitude can be simulated by inserting a varying number of polythene sheets between the source and detector (see Appendix B).

The simulated altitudes with different numbers of sheets are shown in Table 1. Details of calculation can be found in Appendices A and B.

Number of sheets	Simulated altitude (m)
0	0
1	10.0
2	20.0
4	39.9
6	59.9
8	80.1

Table 1: Simulated altitude as a function of number of polythene sheets.

4.2 Using singular value decomposition to determine standard spectra over a range of simulated detector heights

As a first step, for each of the three radio elements K, U and Th, we organize the height dependent spectra in matrices S_{ij}. Rows i and columns j in these matrices correspond to the simulated heights and the energy channels, respectively, and the spectra for zero height are placed in the first row $i = 1$.

To separate the signal from the noise content of the spectra we then apply a singular value decomposition (SVD) on the matrices $\mathbf{S} \in \mathrm{R}^{N_{Height}\, x\, M_{Channel}}$ with $\mathrm{N}_{\mathrm{Height}} < \mathrm{M}_{\mathrm{Channel}}$

$$S_{jk} = \mathbf{S} = \mathbf{U}\Sigma\mathbf{V}^{\mathbf{T}} = \sum_{i=1}^{N_{Height}} \underbrace{\lambda_i \mathbf{u}_i \mathbf{v}_i^T}_{F_{jk}^{(i)}} \qquad (1)$$

The columns of the matrices **U** and **V** consist of mutually orthogonal unit vectors $\mathrm{U} = (\mathrm{u}_1, ..., \mathrm{u}_{N_{Height}})$ and $\mathrm{V} = (\mathrm{v}_1, ..., \mathrm{v}_{M_{Channel}})$ and Σ is a diagonal matrix, whose diagonal elements λ_i are arranged in decreasing order. It can be easily shown that λ_i^2 are the eigenvalues of the matrix product $\mathbf{S}^T\mathbf{S}$. An important property of singular value decomposition is that the matrix **S** can be split into a sum of N_{Height} matrices $F_{jk}^{(i)}$. These matrices $\mathbf{F}^{(i)}$ are called "outer product eigenimages" and the associated vectors v_i "principal components".

For our matrices **S** the first two eigenimages already contain the most pronounced characteristics of the height dependent spectra. In Figure 8 for example we see that the first two eigenimages include almost the complete signal content of the height simulated potassium spectra, whereas the remaining eigenimages contain mostly noise. In the same way the signal content of the height simulated spectra of uranium and thorium are accumulated in the first two eigenimages (Figure 9 and Figure 10). For this reason we have used only the spectral contributions of the first two eigenimages for construction of height dependent U, K and Th standard spectra.

4.3 Use of a global search algorithm to find scaling parameters for flexible height dependent K, U and Th standard spectra

To obtain standard spectra as a function of height we have adapted the work of Dickson (1980), who observed that height variable standard spectra $\mathrm{s}(h)$ can be expressed as a linear combination of the first two principal components v_1 and v_2 at zero height, and two functions a and b that are dependent only on the height h:

$$\mathbf{s}(h) = a(h)\mathbf{v}_1 + b(h)\mathbf{v}_2 \qquad (2)$$

where $a(h)$ and $b(h)$ vary according to the relationships

$$a(h) = A_1 e^{-\mu_1 h} + C_1 \qquad (3a)$$

and

$$b(h) = A_2 e^{-\mu_2 h} + C_2 \qquad (3b)$$

and where the parameters $A_1, A_2, C_1, C_2, \mu_1, \mu_2$ are significantly different for each of K, U and Th. Dickson determined adequate values for these parameters with a Monte Carlo method by fitting the linear combination of the principal components to the corresponding height simulated spectra, and hence obtained expressions for simulated spectra as a function of height.

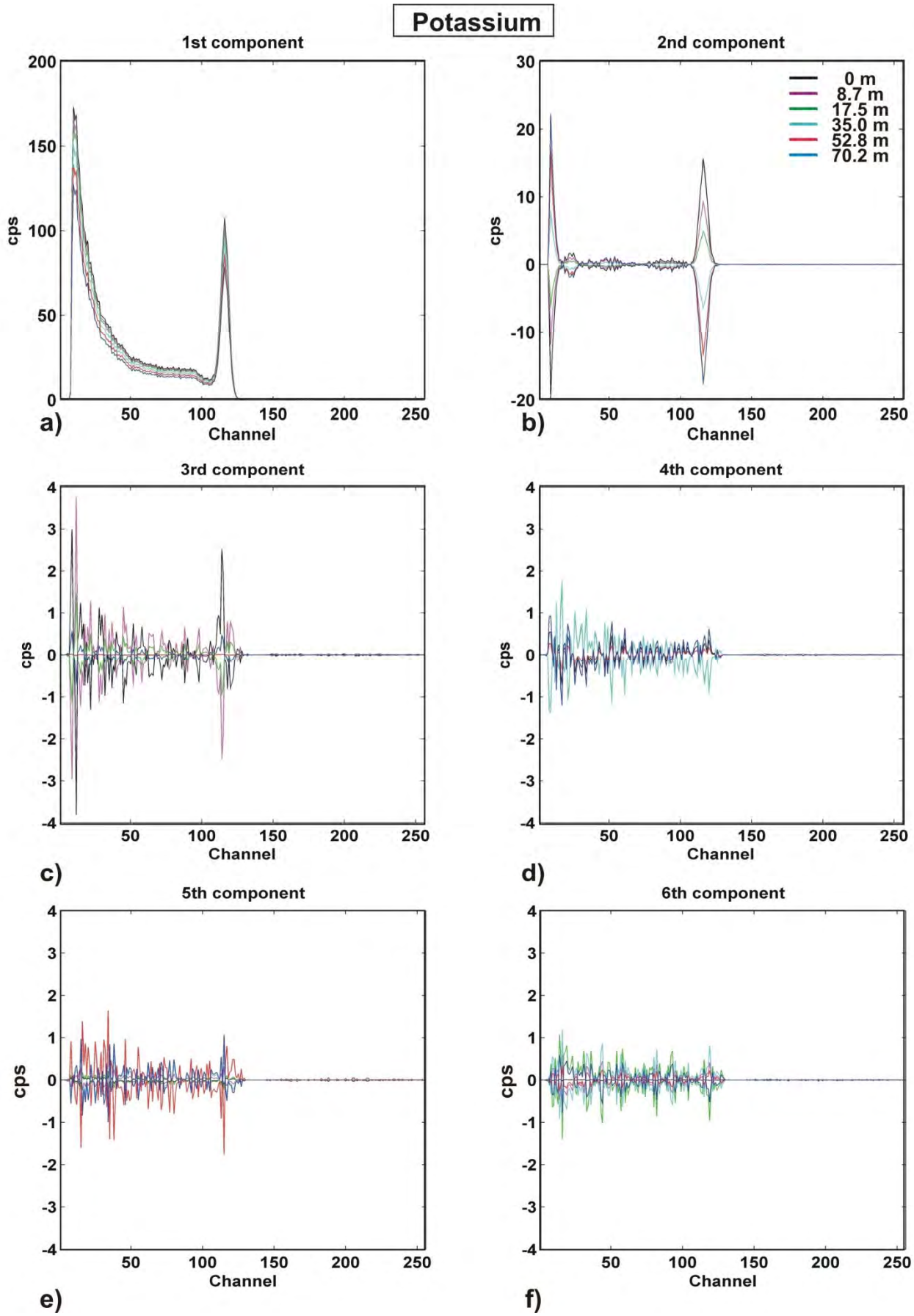

Figure 8: Parts of the height dependent potassium spectra associated with all six eigenimages.

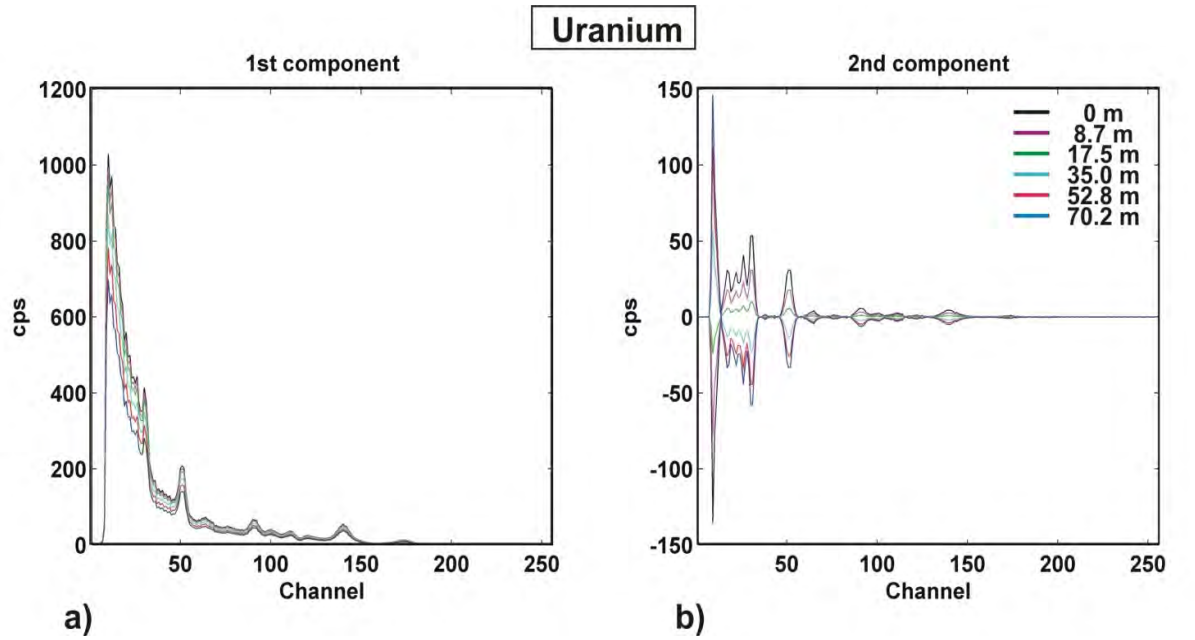

Figure 9: Part of the height dependent uranium spectra associated with the a) first and b) second eigenimages

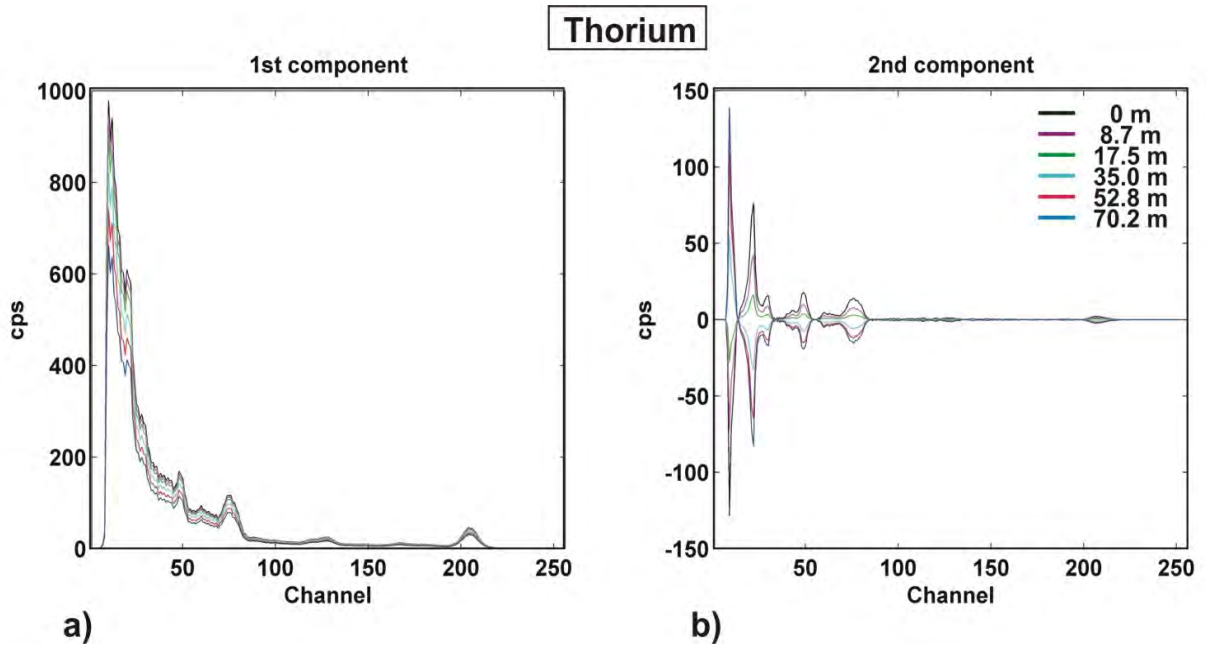

Figure 10: Part of the height dependent thorium spectra associated with the a) first and b) second eigenimage.

Our approach here is similar, but instead of the principal components **v** we have used the rows of eigenimages for the fitting procedure. For each standard spectrum (K, U and Th) the two objective functions θ_1 and θ_2 with

$$\theta_i = \sum_{j=2}^{N_{height}} \sum_{k=1}^{N_{Channels}} (F_{1k}^{(i)} (A_i e^{-\mu_i h_j} - C_i) - F_{jk}^{(i)})^2 \qquad \text{for i = 1,2} \qquad (4)$$

were minimized by varying the parameters $A_1, A_2, C_1, C_2, \mu_1, \mu_2$. The resulting first row of the *i*-th eigenimage $F_{1k}^{(i)}$ corresponds to the spectral contribution at zero height and the other rows

$F_{jk}^{(i)}$ correspond to the spectral contributions at the simulated heights h_j. For the global search we used the Metropolis algorithm (see e.g. Mosegaard and Tarantola, 1995). About 500.000 individual steps in the model space were performed for each objective function. If a region with particularly low misfits was identified for an objective function, the size of the investigated model space was restricted to this region to perform a more local search. Computation for each objective function took 10 to 15 minutes on a conventional PC.

4.4 Resulting flexible height dependent K, U and Th spectra

The parameter combinations of $A_1, A_2, C_1, C_2, \mu_1, \mu_2$ for K, U and Th that provided the ten best fitting results are listed in Appendix C together with their associated RMS errors. To get an idea of the linear dependency of the parameters and the uniqueness of the solution, we plotted the parameters for the ten best fitting results for the K, U and Th standard spectra against each other (Figures 11-13). We see a clear correlation across *A*, *C* and μ for both eigenimages and for all three standard spectra. Such behavior is not surprising when we consider the appearance of equations 3a and 3b. Moreover, relatively large spreading of the parameters with a good data fit indicate that parameter combinations explaining the height dependence of K, U and Th standard spectra are rarely unique for the eigenimages. A probable reason for this is that the simulated height range (up to ~80 m) is not particularly large, and hence variations of the standard spectra are relatively small, and so height dependent characteristics of the spectra are relatively unpronounced.

Because of the non-uniqueness one may question the reliability of the obtained height-dependent spectra. On the other hand we can see from Figures 14-16 that the spectral components of the first two eigenimages at zero height fit very well to the same spectral components at all simulated heights for the parameter combinations with the best fits. Even more importantly, the reconstructed spectra (calculated by equation 2) match well with the processed standard K, U and Th spectra (which were used as input for the singular value decomposition) for all simulated heights. In Figures 17-19 there is little difference between the reconstructed and the processed standard spectra, regardless of the simulated height. Only when we plot the differences between the reconstructed and processed standard spectra do we observe small differences of up to ~5 cps (Figs 20-22). These differences are mainly present in the low energy part, where Compton scattering dominates, but also for some of the most significant photopeaks (e.g. the K-40 photopeak in Fig. 20). Potential reasons for these discrepancies can be that 1) higher eigenimages include some signal content or 2) the global search algorithm was stopped too early to come close enough to the global minima.

We conclude that the linear combination of the spectral components of the first two eigenimages at zero height and with appropriate scaling parameters allow us to create reliable height-dependent U, K and Th standard spectra up to a height of ~ 80 m. Because of the significant spreading of the parameters for combinations with good data fit, we do not recommend using the obtained height-dependent standard spectra for altitudes much larger than 80 m. For most helicopter-borne surveys, flight heights are rarely significantly above 80m. Data sets from airplanes, however, are usually collected at larger altitudes. We therefore recommend that, for airplane data, these height simulation measurements should be repeated with larger simulated heights.

4.5 Relating the cps of the height simulated standard spectra to ground concentrations

To normalize our spectral components from K, U and Th to standard concentrations, the counts-per-second (cps) has to be divided by the ground concentrations of the associated pads. In addition, the spectral components should be multiplied with a factor accounting for the non-infinite nature of the calibration pads. Referring to a description of pads:

- K-40 pad has an average potassium concentration of 6.64 %
- U-238 pad has an average uranium concentration of 52.35 ppm U
- Th-232 pad has an average thorium concentration of 107.72 ppm Th
- The geometric correction factor varies between 1.16 and 1.19

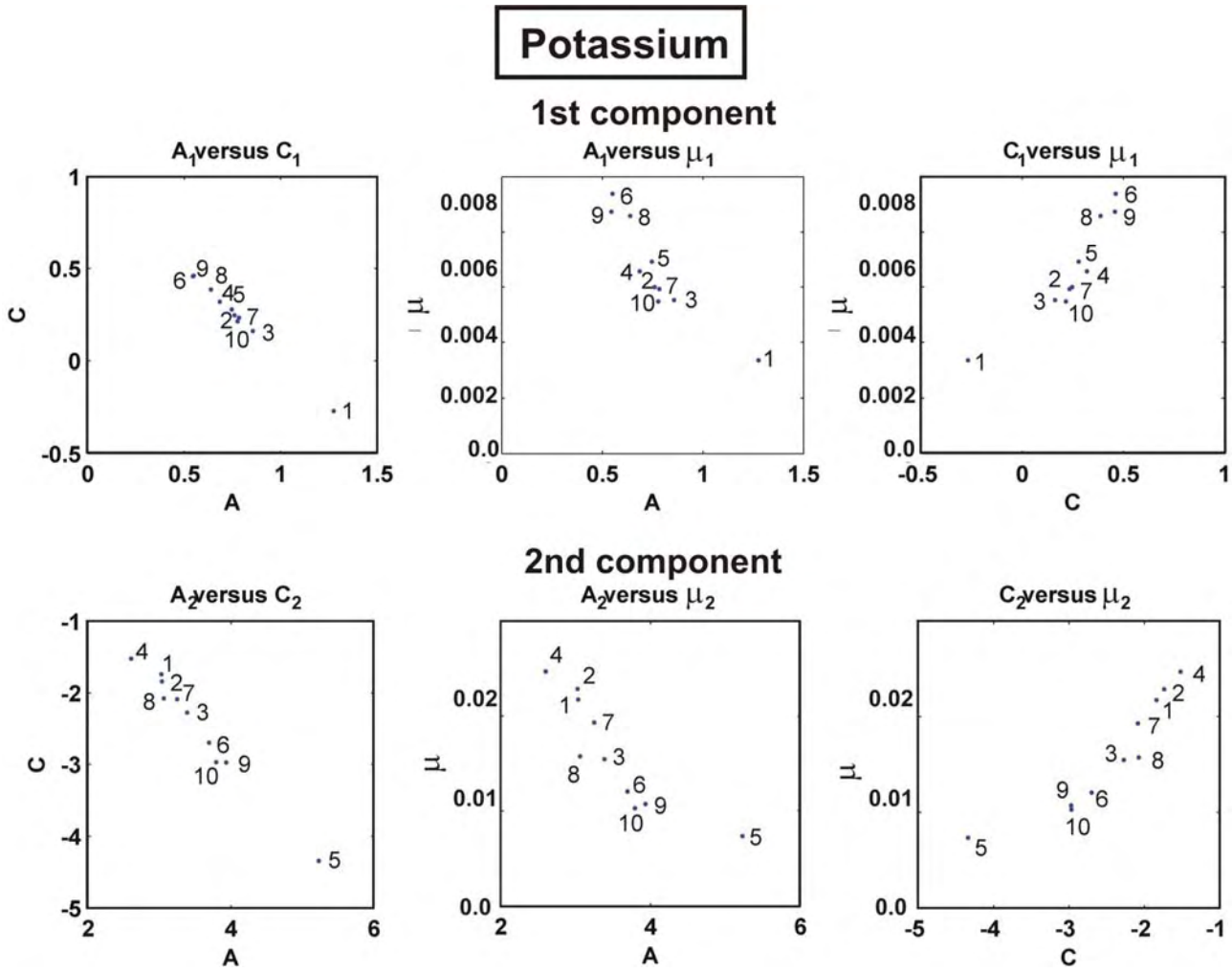

Figure 11: Determined parameter combinations of $A_1, A_2, C_1, C_2, \mu_1, \mu_2$ for the ten best fitting results of global inversion scheme to obtain height variables for K standard spectra.

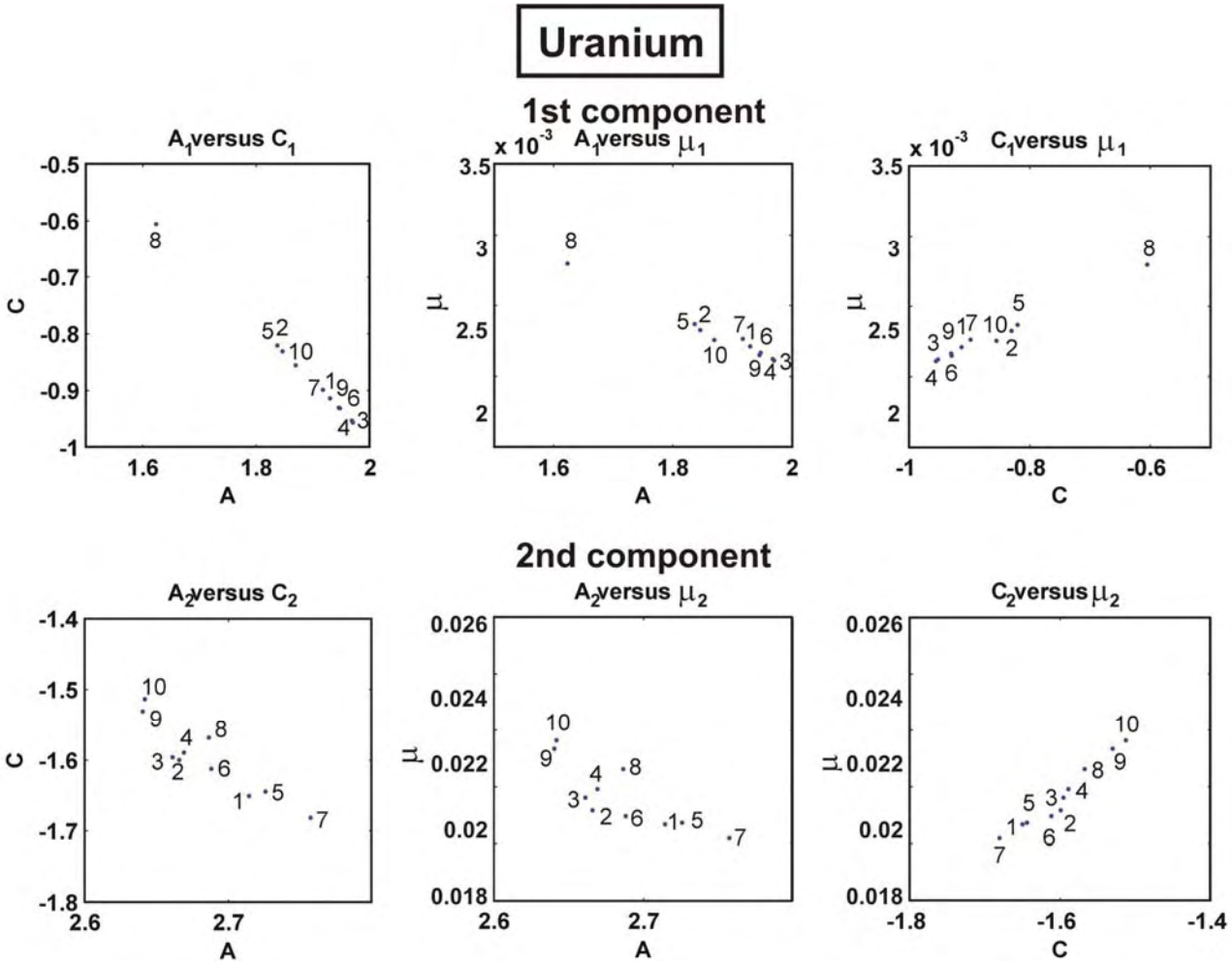

Figure 12: Determined parameter combinations of $A_1, A_2, C_1, C_2, \mu_1, \mu_2$ for the ten best fitting results of the global inversion scheme to obtain height variables for U standard spectra.

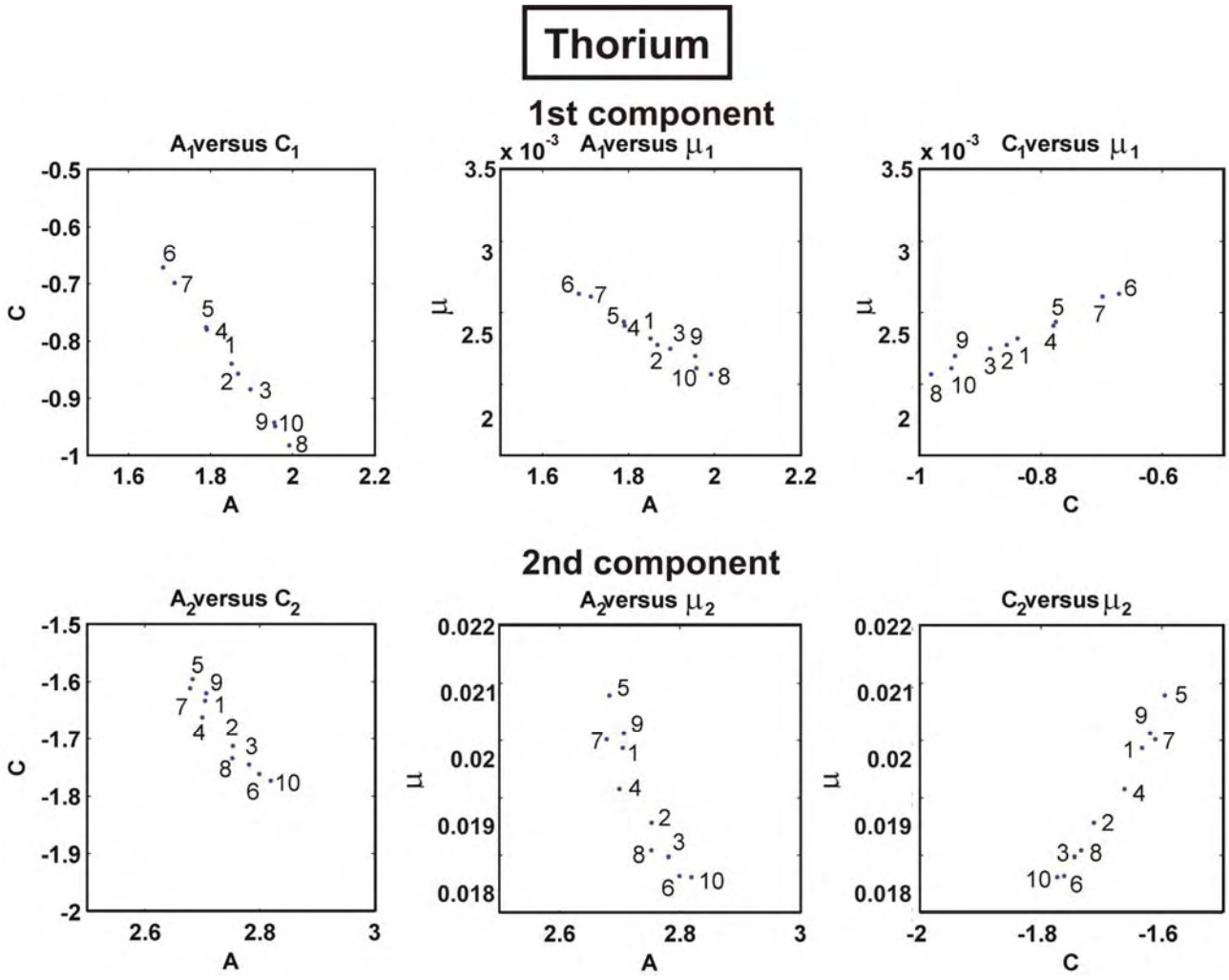

Figure 13: Determined parameter combinations of $A_1, A_2, C_1, C_2, \mu_1, \mu_2$ for the ten best fitting results of the global inversion scheme to obtain height variables for Th standard spectra.

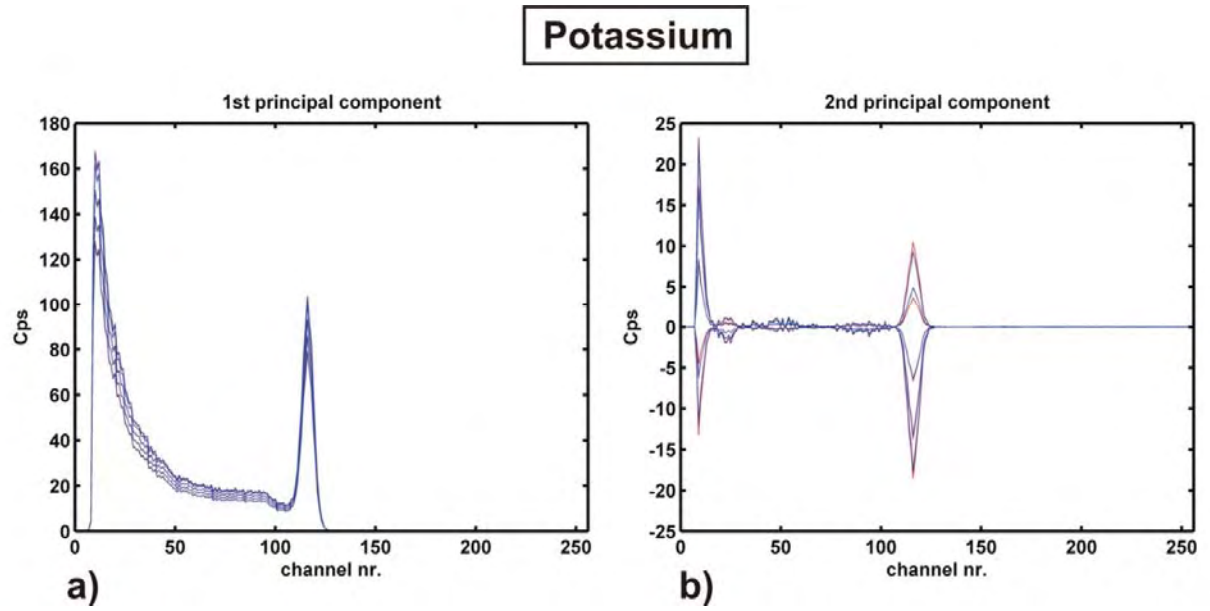

Figure 14: Best results of global inversion scheme to find parameters such that the first row associated with zero height spectra for the a) first and b) second eigenimage of the potassium spectrum fits spectral contributions from the other rows associated with simulated heights of 10.0, 20.0, 39.9, 59.9 and 80.1 meters. Blue lines show the spectral contributions of the eigenimages at different simulated heights. Red lines show the corresponding best fitted spectra obtained with the parameters A1= 1.2756, C1= -0.2686, μ1= 0.002933, A2= 3.0321, C2= -1.8390, μ2= 0.019059 and the spectral contribution of the eigenimages at zero height.

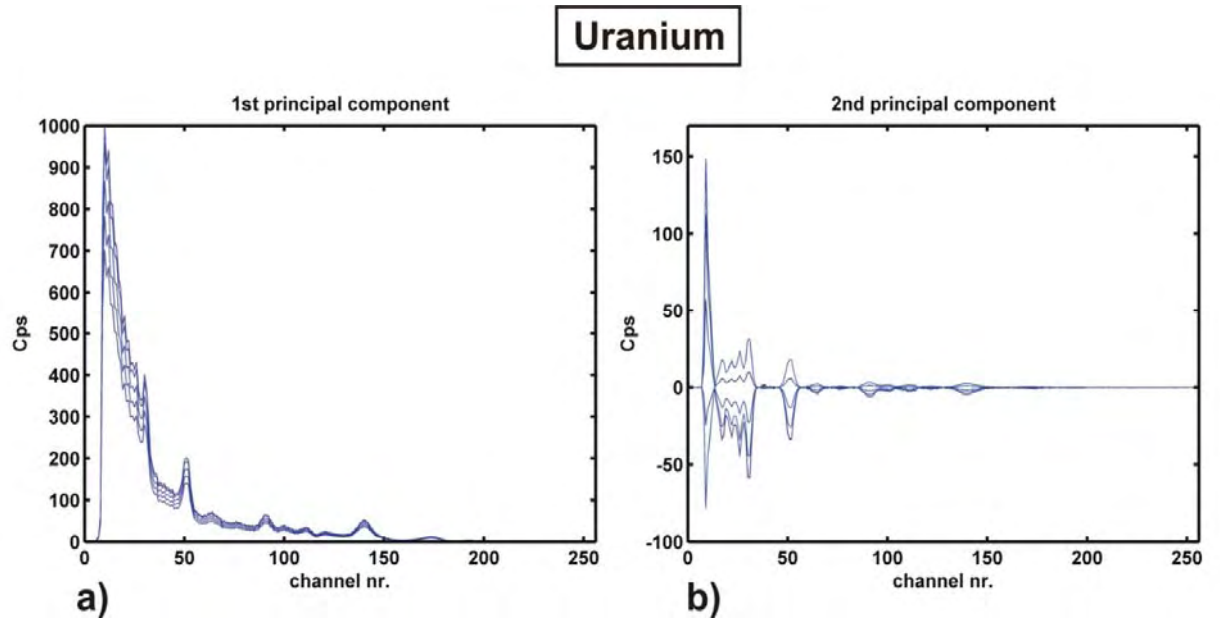

Figure 15: Best results of global inversion scheme to find parameter such that the first row associated with zero height spectra for the a) first and b) second eigenimage of the uranium spectrum fits spectral contributions from the other rows associated with simulated heights of 10.0, 20.0, 39.9, 59.9 and 80.1 meters. Blue lines show the spectral contributions of the eigenimages at different simulated heights. Red lines show the corresponding best fitted spectra obtained with the parameters A1= 1.9297, C1= -0.9134, μ1= 0.002375, A2= 2.7143, C2= -1.6506, μ2= 0.019868 and the spectral contribution of the eigenimages at zero height.

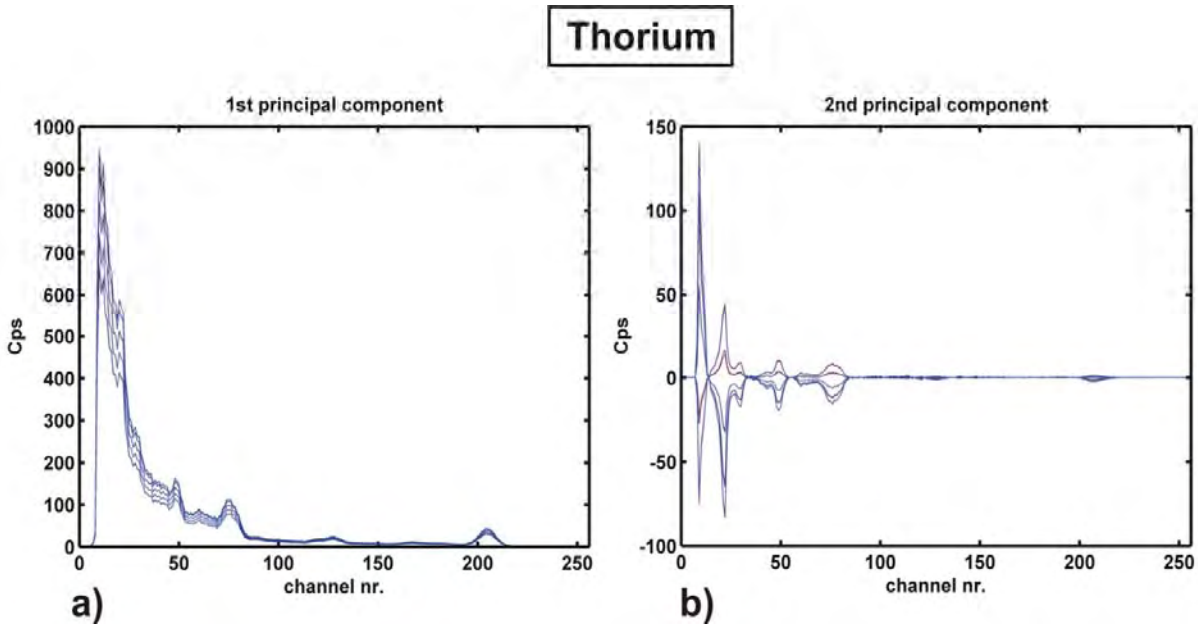

Figure 16: Best results of global inversion scheme to find parameter such that the first row associated with zero height spectra for the a) first and b) second eigenimage of the thorium spectrum fits spectral contributions from the other rows associated with simulated heights of 10.0, 20.0, 39.9, 59.9 and 80.1 meters. Blue lines show the spectral contributions of the eigenimages at different simulated heights. Red lines show the corresponding best fitted spectra obtained with the parameters A1= 1.8511, C1= -0.8392, μ1= 0.002469, A2 = 2.7049, C2= -1.6330, μ2= 0.020036 and the spectral contribution of the eigenimages at zero height.

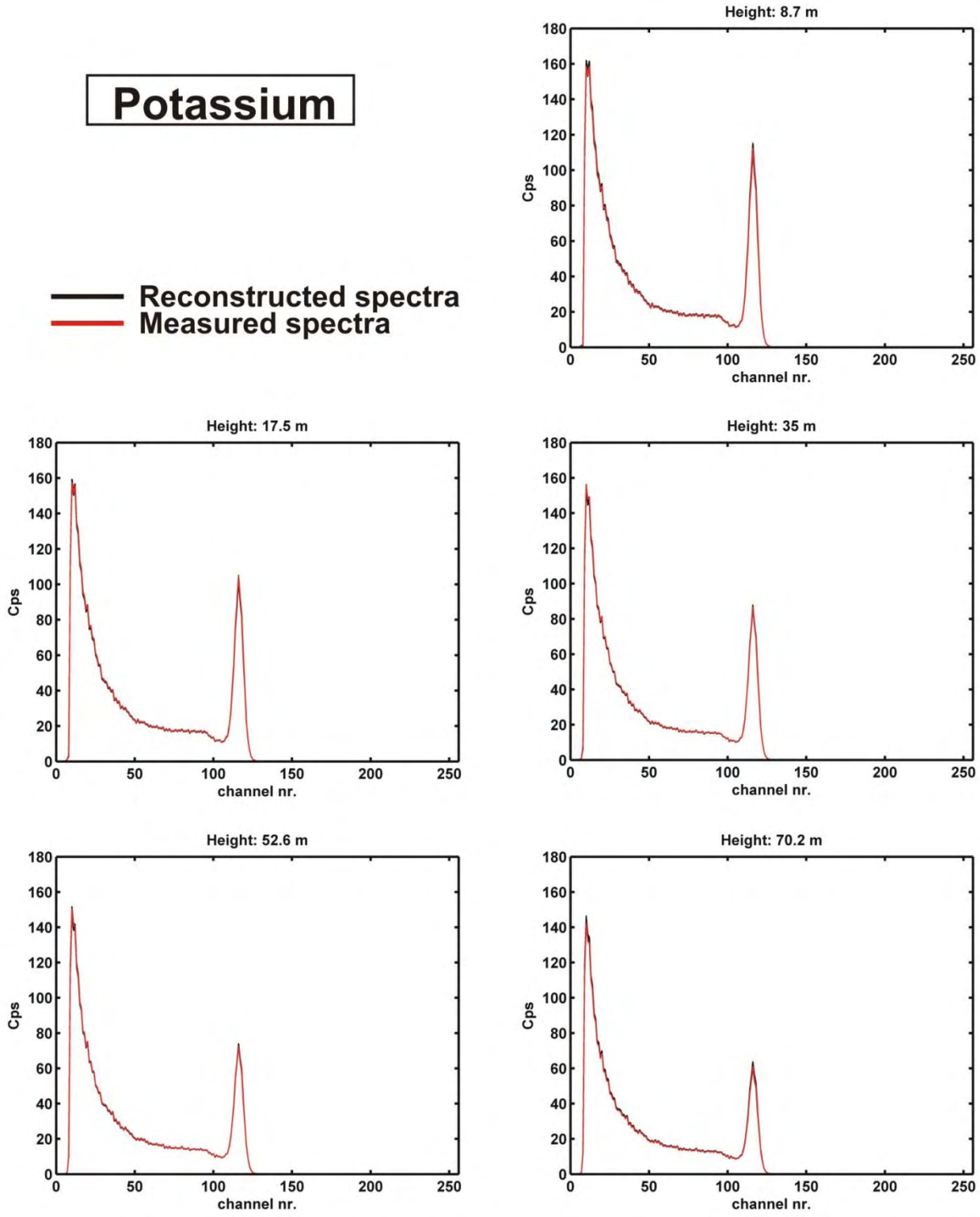

Figure 17: Comparison of measured (processed) and reconstructed potassium spectra at different simulated heights. Black lines show the reconstructed spectra using the spectral contribution of the first two eigenimages associated with zero height and parameter combinations that had the best data fit in the global inversion scheme.

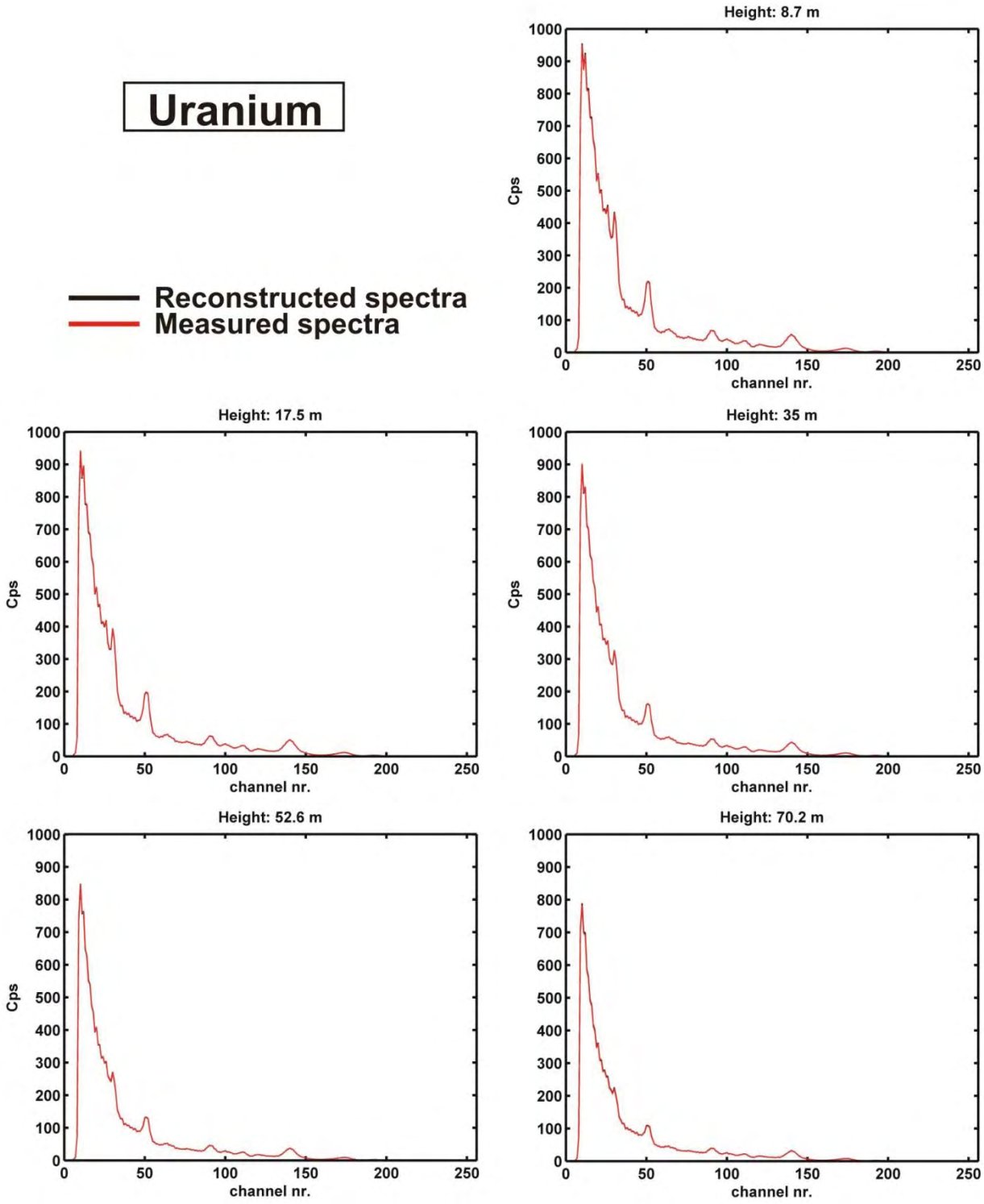

Figure 18: Comparison of measured (processed) and reconstructed uranium spectra at different simulated heights. Black lines show the reconstructed spectra using the spectral contribution of the first two eigenimages associated with zero height and parameter combinations that had the best data fit in the global inversion scheme.

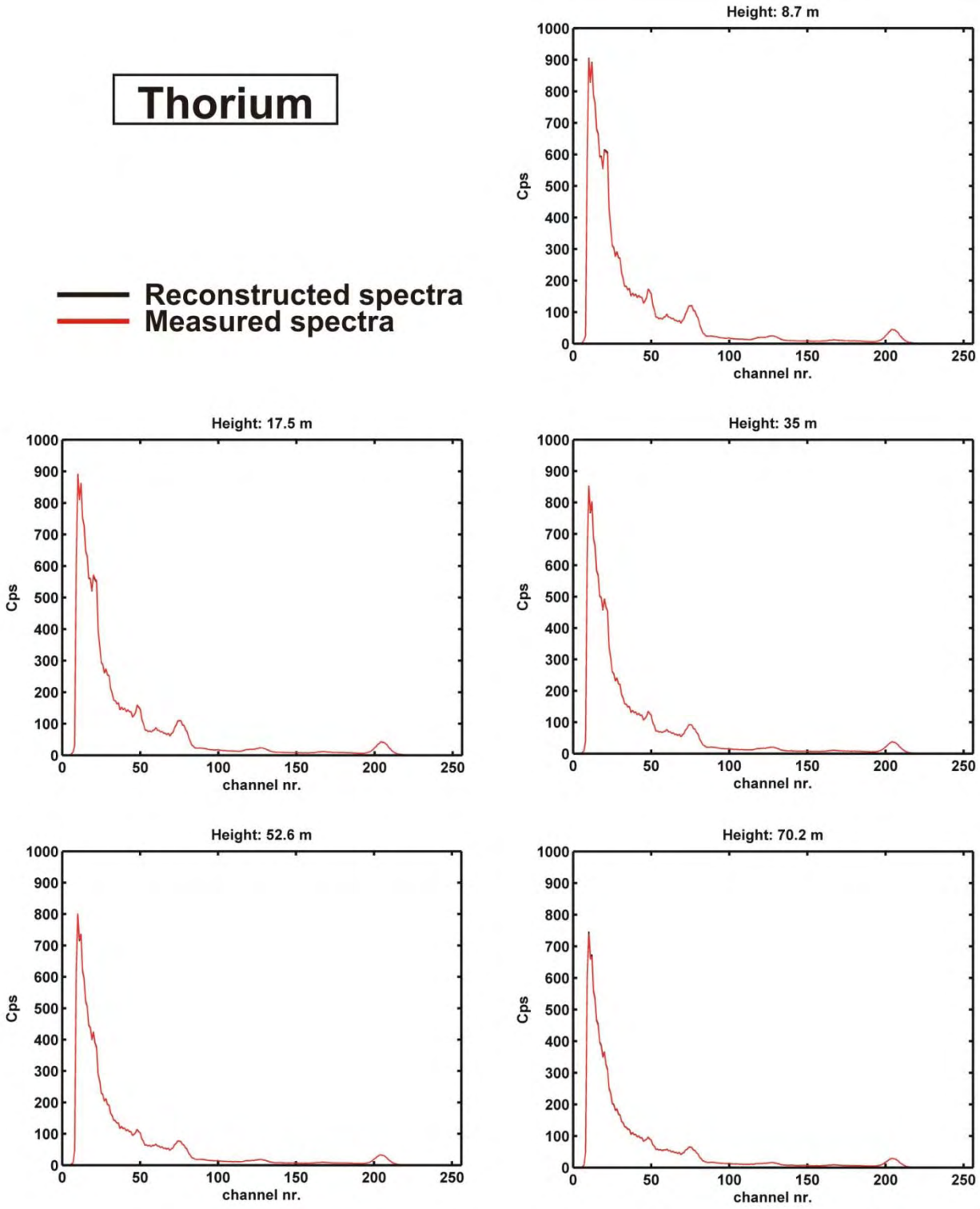

Figure 19: Comparison of measured (processed) and reconstructed thorium spectra at different simulated heights. Black lines show the reconstructed spectra using the spectral contribution of the first two eigenimages associated with zero height and parameter combinations that had the best data fit in the global inversion scheme.

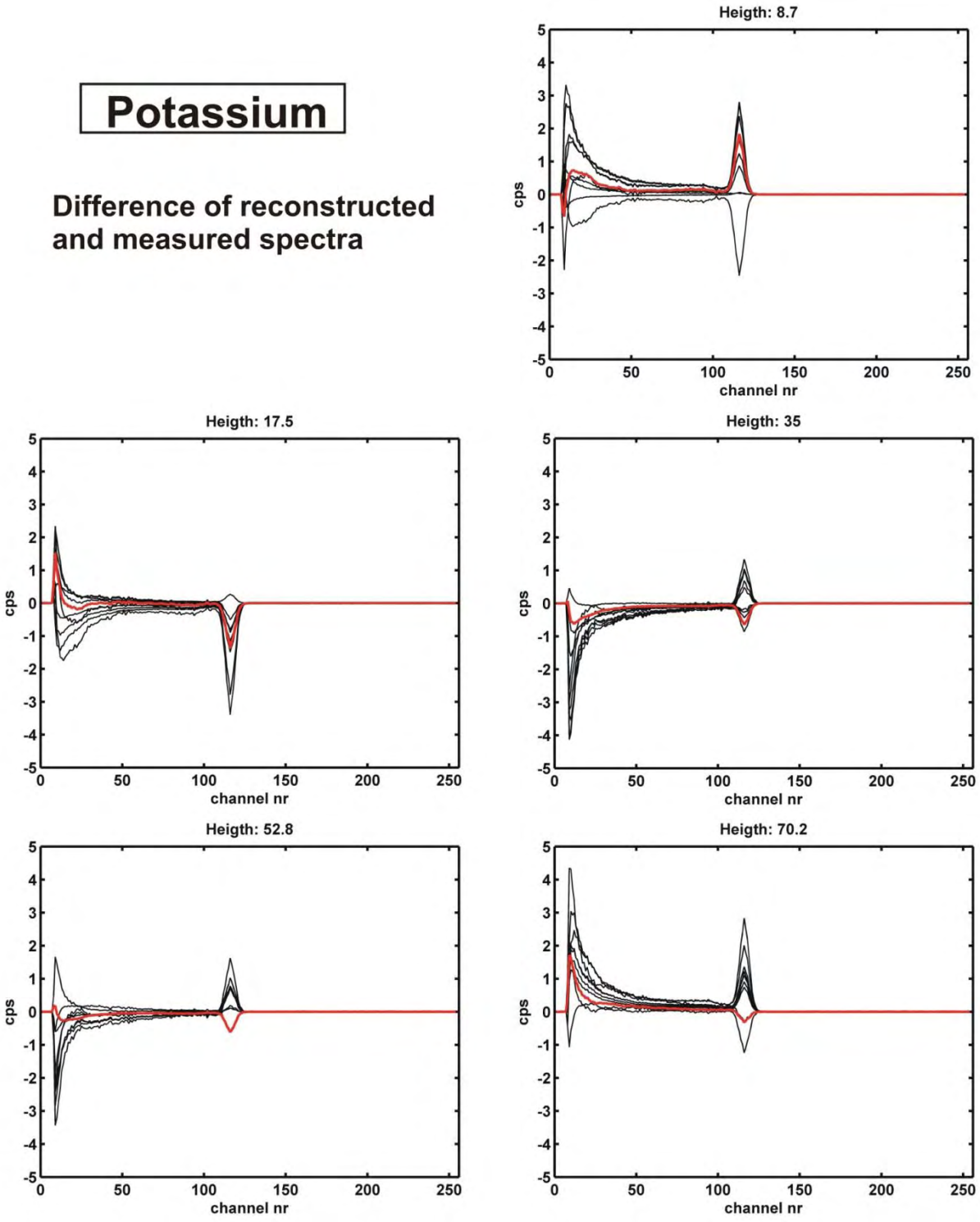

Figure 20: Difference of reconstructed and measured (processed) potassium spectra at different simulated heights. The black lines show the differences for the ten best data fit and the red lines highlight differences for the very best data fit.

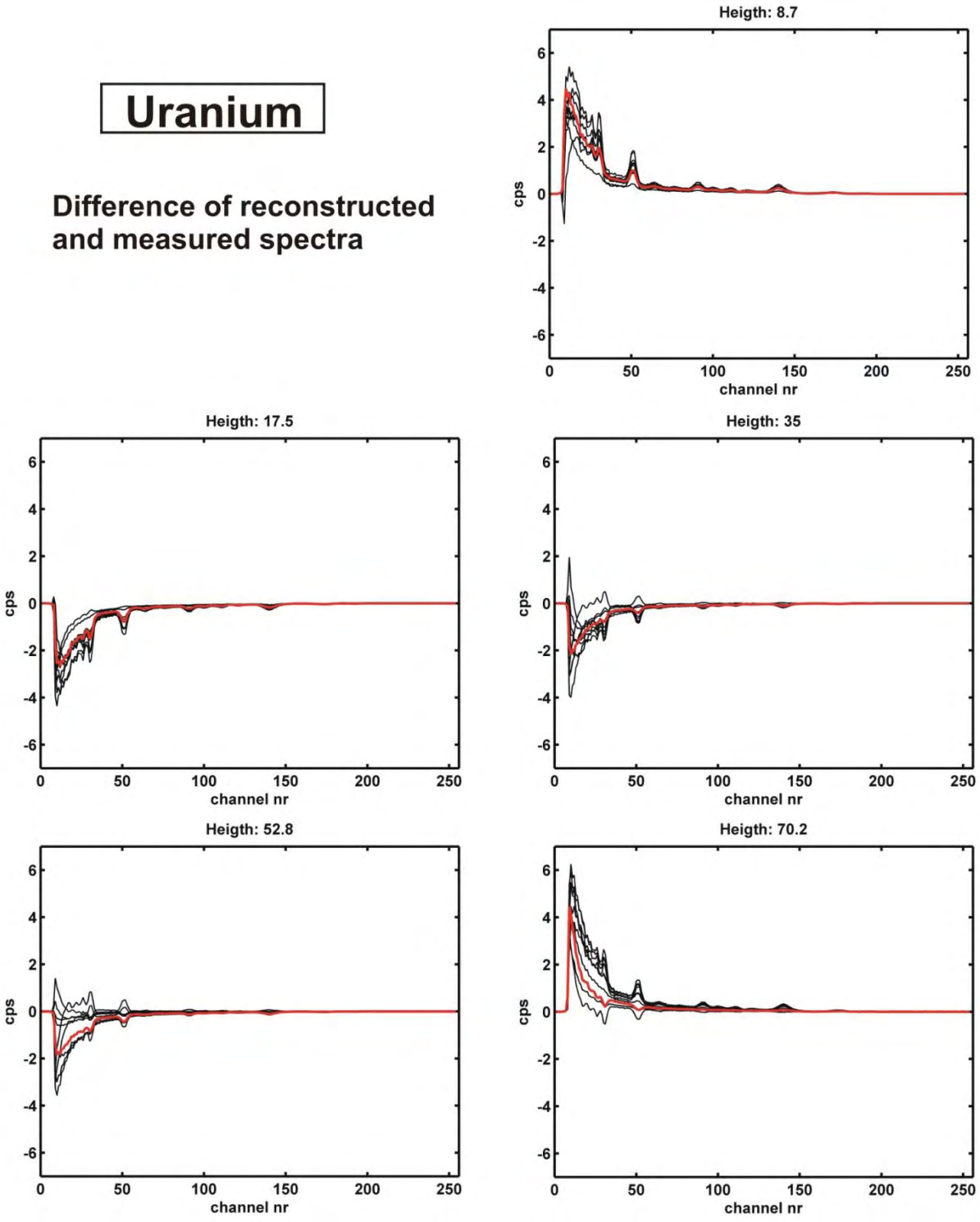

Figure 21: Difference of reconstructed and measured (processed) uranium spectra at different simulated heights. The black lines show the differences for the ten best data fit and the red lines highlight differences for the very best data fit.

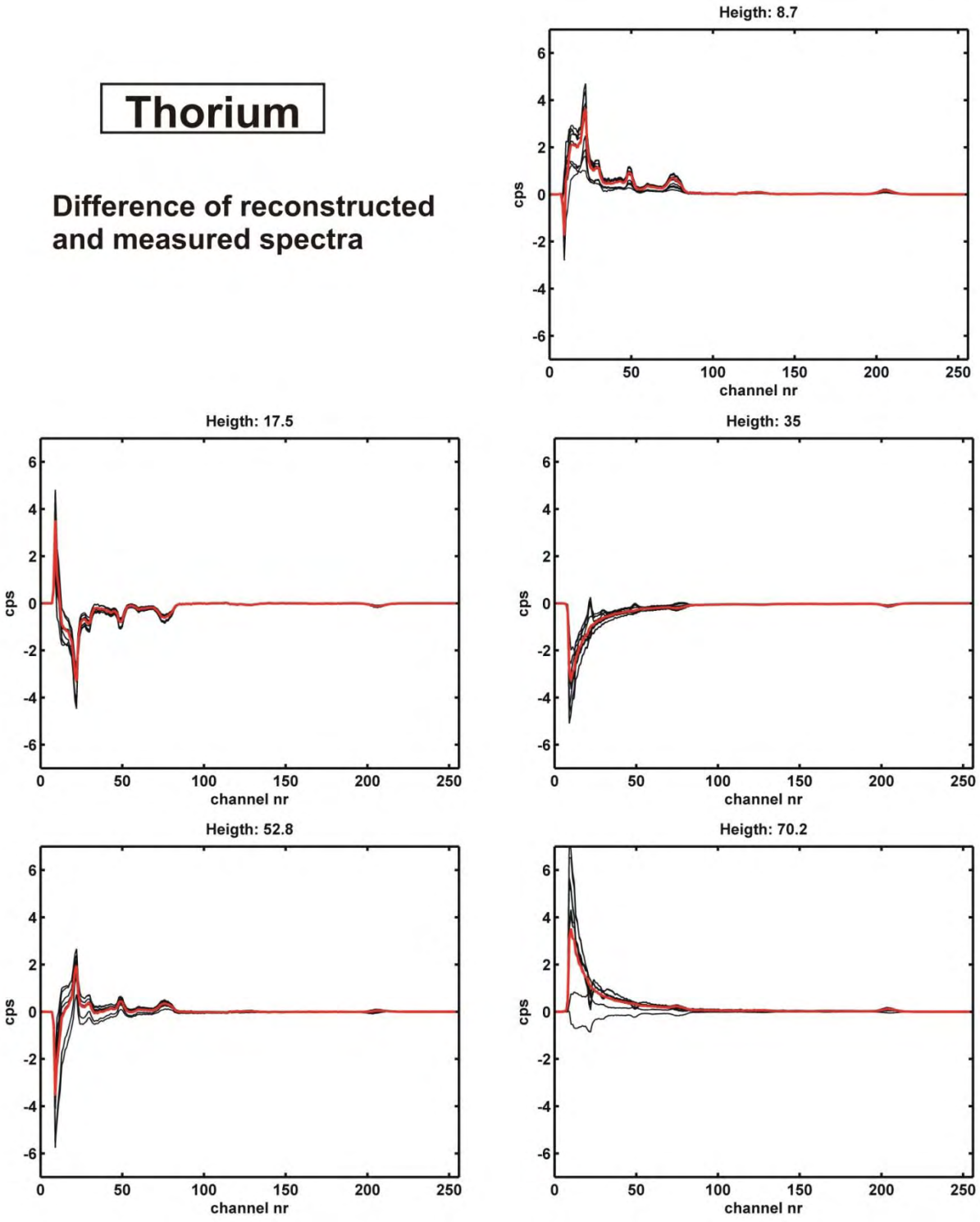

Figure 22: Difference of reconstructed and measured (processed) thorium spectra at different simulated heights. The black lines show the differences for the ten best data fit and the red lines highlight differences for the very best data fit.

4.6 Determination of the height dependence of the stripping ratios

In conventional window-based processing, determination of K, U and Th concentrations is carried out by summing the counts in windows around the energy channel of the most pronounced photopeaks of the associated decay series or radioelements. Usually the following photopeaks are used:

Decay series or radioelement	Nuclide of the used photopeak	Energy of the photopeak in MeV	Energy range of window in MeV
Uranium-238	Bismuth-214	1.76	1.66 – 1.86
Thorium-232	Thalium-208	2.62	2.41 – 2.81
Potassium-40	Potassium-40	1.46	1.37 – 1.57

Table 2: Photopeaks and windows for the natural U, Th and K decay series.

The total counts in each window can be converted to concentrations, assuming one has knowledge of the sensitivity for each radionuclide.

However, because of the Compton scattering continuum and overlap of energy ranges from photopeaks of different decay series, K, U and Th window are "contaminated" with counts that do not originate from their particular radioelement or decay series (e.g. IAEA, 2003). For example, thorium series gamma rays appear in both the uranium and potassium window, and uranium series gamma rays appear in the potassium window. The stripping corrections are applied to correct the window count rates for these "contaminating" counts. The corrections are applied as follows:

$$T_C = \frac{T(1-g\gamma)+U(b\gamma-a)+K(ag-b)}{A} \qquad (5)$$

$$U_C = \frac{T(g\beta-\alpha)+U(1-b\beta)+K(b\alpha-g)}{A} \qquad (6)$$

$$K_C = \frac{T(\alpha\gamma-\beta)+U(\alpha\beta-\gamma)+K(1-\alpha\gamma)}{A} \qquad (7)$$

where $A = 1-g\gamma-a(\alpha-g\beta)-b(\beta-\alpha\gamma)$ (8)

(see for example Grasty, 1977)

T , U and K are the uncorrected counts in the Thorium, Uranium and Potassium windows, and T_C , U_C and K_C are their corrected equivalents. α, β, γ, a, b, and g are the "stripping ratios", and are defined as follows:

- α is the counts in the U window per unit counts in the Th window for a pure Th source
- β is the counts in the K window per unit counts in the Th window for a pure Th source

- γ is the counts in the K window per unit counts in the U window for a pure U source
- *a* is the counts in the Th window per unit counts in the U window for a pure U source
- *b* is the counts in the Th window per unit counts in the K window for a pure K source
- *g* is the counts in the U window per unit counts in the K window for a pure K source

The stripping ratios are usually determined with small calibration pads (such as those available at NGU) with the spectrometer placed directly onto the pads. For NGU's spectrometer system, such calibration parameters were determined initially by the spectrometer manufacturer, and have been repeated by NGU personnel in 2002, 2005 and 2008.

All these calibration measurements determine the stripping ratios at zero height. However, in the literature it is noted that stripping ratios vary significantly with height (IAEA 1991, Allyson and Sanderson 2001). We have therefore used our height simulation data to determine height dependent stripping ratios. For calculation of the stripping ratios we used the processed standard spectra after correcting for live time, background counts, and applying the geometrical factors.

Results for stripping factors as a function of simulated altitude are shown in Tables 2 and 3, and in Figure 23. Stripping ratios for the Cs window are also calculated.

Table 2: Counts per second from Cs, K, U and Th windows for all 3 standard spectra. Altitudes were simulated by the use of plastic sheets.

	0 sheets	1 sheet	2 sheets	4 sheets	6 sheets	8 sheets
Simulated altitude	0 m	10.0 m	20.0 m	39.9 m	59.9 m	80.1 m
Potassium pad						
Cs window	208.97	200.04	194.40	183.66	174.3763981	160.0524
K window	880.24	805.31	745.22	626.42	531.2137316	451.8524
U window	0.05	0.00	0.00	0.04	0.00	0.049161
Th window	0.135614925	0.319025655	0.1170758	0.2969208	0.534232021	0.065343
Uranium pad						
Cs window	1102.80	1023.23	946.96	804.33	691.186901	592.7041
K window	447.55	420.12	394.64	346.99	303.9095306	269.0431
U window	606.67	561.99	521.73	446.37	387.2253858	335.4726
Th window	34.37829293	31.72026906	29.671946	26.096553	23.65674819	19.51556
Thorium pad						
Cs window	847.3790623	797.7346102	755.45311	671.82179	604.7149909	535.0813
K window	299.0114349	288.7885584	277.85426	249.84825	224.1386862	201.075
U window	183.0933242	171.4643223	167.60361	153.04958	141.5437085	127.7309
Th window	577.8246899	539.0360076	513.61959	448.17464	399.6769184	358.4649

Table 3: Stripping ratios as a function of height.

	0 sheets	1 sheet	2 sheets	4 sheets	6 sheets	8 sheets
Simulated altitude	0 m	10.0 m	20.0 m	39.9 m	59.9 m	80.1 m
Alpha	0.3169	0.3181	0.3263	0.3415	0.3541	0.3563
Beta	0.5175	0.5358	0.5410	0.5575	0.5608	0.5609
Gamma	0.7377	0.7476	0.7564	0.7774	0.7848	0.8020
A	0.0567	0.0564	0.0569	0.0585	0.0611	0.0582
B	0.0002	0.0004	0.0002	0.0005	0.0010	0.0001
G	0.0001	0.0000	0.0000	0.0001	0.0000	0.0001
K in Cs-137 window	0.2374	0.2484	0.2609	0.2932	0.3283	0.3542
U in Cs-137 window	1.8178	1.8207	1.8150	1.8019	1.7850	1.7668
Th in Cs-137 window	1.4665	1.4799	1.4708	1.4990	1.5130	1.4927

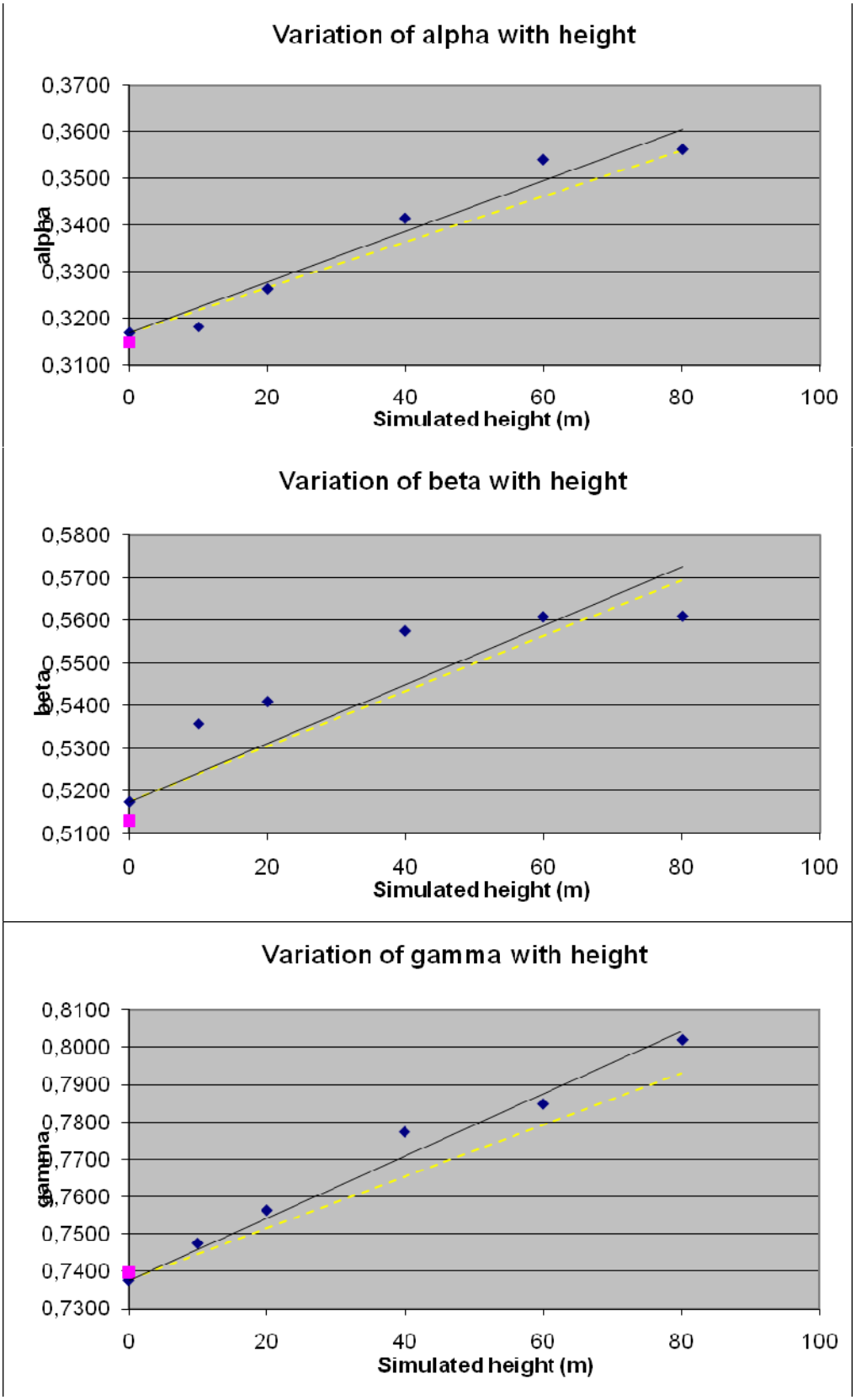

Figure 23: Variation of the stripping parameters α, β and γ with simulated height. Blue dots show stripping parameters determined from our experiment. The black line represents a best-fit to our data points, and fixing the intercept to our zero-height values. The yellow dashed line represents the height dependent relationship suggested by the IAEA (1991), also fixing the intercept to our zero-height values. The purple dots show the stripping parameters determined by calibration measurements with the same pads in August 2008.

The resultant height-dependence of stripping ratios, when using our zero-height value to fix the intercept, are 0.00054 m^{-1}, 0.00069 m^{-1} and 0.00083 m^{-1} for alpha, beta and gamma respectively. Fig.23 also shows the IAEA (1991) gradients (0.00049 m^{-1} 0.00065 m^{-1} and 0.00069 m^{-1}), again using our zero-height value to fix the intercept. Our measured height-dependencies are in reasonable agreement with these from IAEA (1991); we note however that there is considerable variation in height-dependence from various experimental, theoretical, and Monte Carlo studies (see for example Allyson and Sanderson 2001). Height dependence of Cæsium-related stripping factors can be found in the spreadsheet on the CD accompanying this report.

5. Data storage

Our measured and processed K, U and Th standard spectra and the associated spectral components of the eigenimages are stored for all simulated heights on a CD accompanying this report.

6. Conclusion

We have performed height simulation measurements to determine height dependent standard spectra and stripping ratios; stripping ratio results are in reasonable agreement with published IAEA values. Our height-dependent standard spectra will facilitate future multichannel processing of helicopter-borne gamma ray spectrometry data collected with NGU's GR820 spectrometer system.

7. Acknowledgements

The authors wish to thank Mark Smethurst for valuable discussions during the calibration measurements, and Tom Jacobsen and Jørn Fornes for forklift driving.

8. References

Allyson, J.D., Sanderson, D.C.W., 1998. Monte Carlo Simulation of Environmental Airborne Gamma-Spectrometry. Journal of Environmental Radioactivity, (38) 259-282.

Allyson, J.D., Sanderson, D.C.W., 2001. Spectral deconvolution and operational use of stripping ratios in airborne radiometrics. Journal of Environmental Radioactivity, (53) 351-363.

Bailey, R.C., 1986. The altitude dependence of terrestrial gamma-ray spectra: A simple model. Geophysics, (51) 2108-2116.

Dickson, B.H., 1980. Analytic methods for multichannel airborne radiometrics. MS thesis, University of Toronto (unpublished).

Dickson, B.H., Bailey, R.C., Grasty, R.L. 1981. Utilizing multi-channel airborne gamma-ray spectra. Canadian Journal of Earth Science, (18), 1793.

Grasty, R.L. 1977 A General Calibration Procedure for Gamma-ray Spectrometers - Project 720084; in Report of Activities, part C; Geol. Survey of Canada, Paper 77-1C.

IAEA, 1991. Airborne Gamma Ray Spectrometer Surveying, Technical Reports Series, No.323, Vienna Austria.

IAEA, 2003. Guidelines for radioelement mapping using gamma ray spectrometry data. IAEA-TECDOC-1363, Vienna, Austria.

Minty, B.R.S., McFadden, P., Kennett, B.L.N. 1998. Multichannel processing for airborne gamma-ray spectrometry. Geophysics. 63. 1971-1985.

Mosegaard,K. and Tarantola, A. 1995. Monte Carlo sampling of solutions to inverse problems. Journal of Geophysical Research. 100. 12,431 – 12,447.

Rønning, J.S. 2008. Atomberedskap: Plan for NGUs aktivitet. NGU Rapport 2008.002

Smethurst, M.A., Mogaard, J.O, Koziel, J. 2005. A mobile gamma ray spectrometer system for nuclear hazard mapping: GAMMALOG v.3.0. NGU Rapport 2005.026

Appendix A: Electron densities of air and polythene

For a molecule, electron density ρ_e can be calculated using

$$\rho_e = \frac{N_A Z}{A}$$

where N_A is Avogadro's number (molecules per mole), Z is the number of electrons per molecule (which can be determined by summing the atomic numbers of the constituent atoms of the molecule), and A is the number of grams per mole (which can be determined by summing the mass numbers of the constituent atoms of the molecule).

Using the above formula, we obtain for air (assuming for our purposes a mixture of 80% N_2 and 20% O_2) an electron density

$$\rho_{e,air} = 3.0 \times 10^{23} electrons / gram$$

and for polythene (treating is as a "molecule" with chemical formula C_2H_4), we obtain

$$\rho_{e,polyethene} = 3.4 \times 10^{23} electrons / gram$$

For many elements, A is approximately twice Z, and so the electron density for many elements and compounds will be close to half the value of Avogadro's number, i.e. $3.0\,x\,10^{23}$ electrons/gram. Significant deviation from this value will only be found if the material contains either heavy elements (for which A > 2Z), or a large proportion of Hydrogen (for which A = Z). Typical substitutes for air used in absorption experiments are plywood, perspex and polythene, all of which contain Hydrogen in varying proportions, and so which have slightly higher electron densities than that of air.

Appendix B: Equivalent thickness of air

Using the Law of Boyle-Mariotte for an isothermal atmosphere we have the following expression for the air pressure *P* as a function of height *h*:

$$P(h) = P_0 e^{Cgh} \qquad \text{(B1)}$$

where P_0 is the pressure at $h = 0$, g is the gravitational constant, and C is a constant relating the relationship between pressure and density, such that

$$\rho(h) = CP(h) \qquad \text{(B2)}$$

C can be determined using standard values of air pressure and density at $h = 0$:

$$C = \frac{\rho_0}{P_0} = \frac{1.29\,kg/m^3}{1.013\times10^5\ N/m^2} = 1.277\times10^{-5}\ \frac{s^2}{m^2} \qquad \text{(B3)}$$

Combining equations (B1) and (B2) we obtain:

$$\rho(h) = \rho_0 e^{Cgh} \qquad \text{(B4)}$$

We wish to calculate the height H of atmosphere such that the mass per unit area is equivalent to the mass per unit area of a number n of plastic sheets.

The mass per unit area of the plastic sheets is given by $nt\rho_{plastic}$ where n is the number of sheets of thickness t, and $\rho_{plastic}$ is the density of plastic.

The mass per unit area of a height of air H must be determined by integration and can be expressed as

$$\int_0^H \rho\ dh \qquad \text{(B5)}$$

Equating the terms we have

$$nt\rho_{plastic} = \int_0^H \rho_0 e^{Cgh}\ dh \qquad \text{(B6)}$$

Solving for H we eventually obtain

$$H(n) = \frac{-1}{Cg}\ln\left(1 - \frac{nt\rho_{plastic}Cg}{\rho_{air}}\right) \qquad \text{(B7)}$$

Introducing a correction factor for the electron densities f, defined as the ratio of the electron density of polythene to the electron density of air (Appendix A), we have:

$$H(n) = \frac{-1}{Cg}\ln\left(1 - \frac{ntf\rho_{plastic}Cg}{\rho_{air}}\right) \qquad \text{(B8)}$$

Equation (B8) was used to calculate the values in Table 1, using $\rho_{air} = 1.29 Kg/m^3$, $\rho_{plastic} = 945 Kg/m^3$, t = 0.012m, g = 9.81ms^{-2}, , $C = 1.277\ x10^{-5}\ s^2/m^2$, and f = 1.133.

Appendix C: Parameter combinations A, C and μ giving the best fitting results for height -dependent K, U and Th standard spectra

Potassium				
Parameters Model	A	C	μ in 1/m	Rms error in cps
For the 1st eigenimage				
1	1.275585	-0.268618	0.002933	5.617340
2	0.760140	0.247057	0.005257	8.603312
3	0.855614	0.161444	0.004841	9.296629
4	0.685223	0.319786	0.005757	11.229920
5	0.746232	0.277944	0.006063	11.640629
6	0.549781	0.461739	0.008223	11.740873
7	0.783097	0.233468	0.005196	12.374492
8	0.638824	0.386970	0.007523	12.636182
9	0.545065	0.457613	0.007657	13.871311
10	0.777244	0.214594	0.004798	14.338215
For the 2nd eigenimage				
1	3.032066	-1.839009	0.019059	5.411146
2	3.025090	-1.738492	0.020043	6.471446
3	3.384858	-2.272199	0.013530	6.974282
4	2.602226	-1.520482	0.021649	7.137373
5	5.227336	-4.341214	0.006437	7.355731
6	3.690258	-2.701254	0.010553	7.369555
7	3.246603	-2.086336	0.016933	7.590464
8	3.060109	-2.075037	0.013770	7.611540
9	3.932865	-2.974086	0.009386	7.805994
10	3.791251	-2.970583	0.009013	8.421025

Table C 1: Parameter combinations with the ten best fitting results to obtain the height variable potassium standard spectrum by the first two eigenimages.

Uranium				
Parameters Model	A	C	μ in 1/m	Rms error in cps
For the 1st eigenimage				
1	1.929666	-0.913393	0.002375	21.365437
2	1.845895	-0.830432	0.002476	22.548054
3	1.969707	-0.955938	0.002287	22.863370
4	1.967703	-0.952663	0.002298	22.970726
5	1.836594	-0.820634	0.002513	23.030573
6	1.947168	-0.930823	0.002336	23.284971
7	1.917139	-0.898714	0.002421	23.462819
8	1.623115	-0.605260	0.002887	24.711431
9	1.945135	-0.929881	0.002322	24.803272
10	1.869079	-0.855472	0.002415	24.812279
For the 2nd eigenimage				
1	2.714260	-1.650565	0.0198677	3.821647
2	2.665671	-1.599676	0.020302	4.112067
3	2.661009	-1.595916	0.020692	4.396688
4	2.668960	-1.589474	0.020951	4.419969
5	2.725714	-1.644477	0.019914	5.162846
6	2.688004	-1.612097	0.020117	6.237353
7	2.757242	-1.681270	0.019442	6.292439
8	2.686359	-1.567951	0.021575	6.407856
9	2.640225	-1.530428	0.022203	6.442131
10	2.641589	-1.512971	0.022468	6.491573

Table C 2: Parameter combinations with the ten best fitting results to obtain the height variable uranium standard spectrum by the first two eigenimages.

Thorium				
Parameters Model	A	C	μ in 1/m	Rms error in cps
For the 1st eigenimage				
1	1.851190	-0.839156	0.002469	15.122007
2	1.867459	-0.856870	0.002430	15.980187
3	1.896868	-0.884100	0.002405	16.035319
4	1.790730	-0.779724	0.002547	16.610972
5	1.789042	-0.775735	0.002571	16.757843
6	1.684138	-0.671510	0.002744	17.108795
7	1.712052	-0.698404	0.002726	17.362767
8	1.991906	-0.981758	0.002250	17.463058
9	1.955401	-0.942316	0.002363	17.729408
10	1.957799	-0.948467	0.002286	18.209457
For the 2nd eigenimage				
1	2.704888	-1.633021	0.020036	11.046080
2	2.753087	-1.712385	0.018894	11.067803
3	2.781058	-1.744885	0.018378	11.155399
4	2.699617	-1.662004	0.019404	11.282050
5	2.682923	-1.595374	0.020844	11.392355
6	2.799349	-1.761495	0.018089	11.693895
7	2.678330	-1.610988	0.020165	11.802667
8	2.752354	-1.733771	0.018471	11.837464
9	2.706739	-1.619837	0.020261	11.846741
10	2.818906	-1.773176	0.018075	11.964791

Table C 3: Parameter combinations with the ten best fitting results to obtain the height variable thorium standard spectrum by the first two eigenimages.

Appendix D: Contents of CD

The CD included with this report contains the following files and folders:

README
Description of CD contents.

PCA_data.m
Matlab script for splitting radiometric spectra into their principal components.

determine_const_PCA.m
Matlab script for determining constants describing height-dependence of standard spectra.

GR820 height-dependent calibrations.xls
Spreadsheet containing calculations and graphs.

raw data
Folder containing raw data files.

raw data\README
Descriptions of raw data files.